Models of fragmentation and partitioning phenomena based on the symmetric group S_n and combinational analysis

A. Z. Mekjian*
Institute of Nuclear Theory, HN-12, University of Washington, Seattle, Washington 98195

S. J. Lee†
Department of Physics and Astronomy, Rutgers University, Piscataway, New Jersey 08855
(Received 6 February 1991; revised manuscript received 10 June 1991)

Various models for fragmentation and partitioning phenomena are developed using methods from permutation groups and combinational analysis. The appearance and properties of power laws in these models are discussed. Several exactly soluble cases are studied. An application to nuclear fragmentation and clusterization is given. A connection with Ewens's approach [Theor. Popul. Biol. **3**, 87 (1972); *Mathematical Population Genetics* (Springer, Berlin, 1979)] to genetic diversity is mentioned. Applications to the social behavior of a vervet monkey troop and to the group behavior of people are given.

PACS number(s): 05.40.+j, 02.50.+s

I. INTRODUCTION

Fragmentation and clusterization phenomena are observed in many different areas of physics. A fragmentation process produces a cluster distribution of objects following a collision or some other method of excitation or deexcitation. The mass or size distribution that results from some types of processes is of interest, and this distribution gives the number of clusters of a given size as a function of their size. Examples are nuclear fragment distributions following a collision of two heavy ions [1], meteoritic distributions reaching the earth [2], earthquake sizes [3], avalanche [4] and sandpile [5] slides, lunar crater sizes [6], percolation cluster distributions [7], droplet sizes [8] in aerosols, and in condensation phenomena. One remarkable feature in these examples is the appearance of a power law in the size distribution. That is, the distribution of sizes falls as a power of the size of the object. Power laws appear in many other areas. Examples are Zipf's law [9] in linguistics for word frequency use, Pareto's law [10] in economics for income distributions, and $1/f$ noise [11]. Moreover, $1/f$ noise appears in many phenomena [5] from starlight flicker to sand flow and traffic flow. A more detailed summary of power laws can be found in Mandelbrot [12] and in Montroll and West [13].

In a previous set of papers [14,15], a model for a fragmentation process was introduced and developed. A connection of this model with a thermodynamical description of a nuclear fragmentation process is given in Ref. [16]. This paper considers further developments, extensions, and applications of this model. The various cases considered all have hyperbolic power-law behavior at some particular point. A link between these models and the symmetric group S_n is developed, and combinational methods are also employed in our studies. Applications of our approach to various fragmentation phenomena and partitioning problems will be given and compared with data.

An outline of this paper is as follows. In Sec. II, a relationship between fragmentation partitions and permutation cycles of the symmetric group S_n is developed. Canonical ensemble partition functions are derived in Sec. III and used to obtain general expressions for the distribution of cluster sizes in fragmentation phenomena and group sizes in partitioning problems. Section IV considers various exactly soluble cases. This model is also related to probability theory. Section V gives some applications of the results developed in Sec. IV. These applications include nuclear fragmentation, the solar abundance of the elements, genetic diversity, and social behavior of a troop of monkeys and people. Section VI is for the concluding remarks. Some generating functions are given in the Appendix.

II. PARTITIONS, DECOMPOSITIONS, FRAGMENTATIONS, AND PERMUTATION CYCLES

In a fragmentation process, an object made of A elements is divided into pieces of smaller size. Specifically, the initial A elements end up in smaller groups or clusters of varying sizes characterized by the number of elements j in the cluster. Here the number of objects of size j is called n_j and a sum rule

$$A=\sum_{j=1}^{A} jn_j \tag{1}$$

exists as a constraint. The listing of the partitions of A objects into such groups also appears in number theory as the decomposition of an integer A into integer summands without regard to order. The integer j will be identified with the cluster of size j. The notation

$$\Pi_A=\Pi_A(\{n_j\})=(1^{n_1},2^{n_2},\ldots,A^{n_A}) =(n_1,n_2,\ldots,n_A) \tag{2}$$

TABLE I. Partitions (Π_A) of $A=5$ and 6. The parity and the Cauchy numbers (M_2) are also given.

A	$p(A)$	m	$p(A,m)$	$\Pi_A(\mathbf{n})$	$\Pi_A(\boldsymbol{\lambda})$	Parity	M_2
5	7	1	1	5	1^5	+	24
		2	2	1,4	$2,1^3$	−	30
				2,3	$2^2,1$	−	20
		3	2	$1^2,3$	$3,1^2$	+	20
				$1,2^2$	3,2	+	15
		4	1	$1^3,2$	4,1	−	10
		5	1	1^5	5	+	1
6	11	1	1	6	1^6	−	120
		2	3	1,5	$2,1^4$	+	144
				2,4	$2^2,1^2$	+	90
				3^2	2^3	+	40
		3	3	$1^2,4$	$3,1^3$	−	90
				1,2,3	3,2,1	−	120
				2^3	3^2	−	15
		4	2	$1^3,3$	$4,1^2$	+	40
				$1^2,2^2$	4,2	+	45
		5	1	$1^4,2$	5,1	−	15
		6	1	1^6	6	+	1

is used to specify a particular decomposition of an integer A, a particular fragmentation of an object made of A elements, or division of A objects into smaller groups. The multiplicity of a given partition is

$$m=n_1+n_2+\cdots+n_A=\sum_{j=1}^{A} n_j \ . \tag{3}$$

The possible values of m are $m=1,2,\ldots,A$. The number of possible partitions of A without regard to order is called $p(A)$ and the number of possible partitions of A into m parts is called $p(A,m)$. Here $p(A)=\sum_{m=1}^{A} p(A,m)$. Table I lists all the partitions for $A=5$ and 6.

For large A, the total number of partitions of A is the Hardy-Ramanujan asymptotic result [17,18]

$$p(A)\approx\frac{1}{4\sqrt{3}A}e^{\pi\sqrt{2A/3}} \ . \tag{4}$$

Also, for large A and $m \ll A$ [$m\sim O(A^{1/3})$],

$$p(A,m)\approx\frac{A^{m-1}}{m!(m-1)!} \ . \tag{5}$$

Generating functions for $p(A)$ and $p(A,m)$ are given in the Appendix.

The $p(A)$ and $p(A,m)$ also appear in level densities. If the number of elements A is replaced by the number of levels g_0E at a given energy E, then substitution of $A=g_0E$ turns Eq. (4) into the level density $\rho(E)$ of a Fermi gas [19] and Eq. (5) into the level density for states made of m particles plus holes [20]. Specifically,

$$\begin{aligned}\rho(E)&=g_0p(A=g_0E)=\frac{1}{4\sqrt{3}E}e^{2(\pi^2g_0E/6)^{1/2}} \ , \\ \rho_m(E)&=g_0p(A=g_0E,m)=g_0\frac{(g_0E)^{m-1}}{m!(m-1)!} \ .\end{aligned} \tag{6}$$

Here the g_0 is the level density parameter. Moreover, a generalization of Eq. (4) can be used to study statistical mechanics of cosmic bosonic strings [21] and the Hagedorn level density of strong interactions [22]. The importance of $p(A)$ here is in counting the number of possible fragmentations. Each fragmentation is specified by $\Pi_A(\{n_i\})$ of Eq. (2) so that $\sum_{\Pi_A} 1=p(A)$, where the sum is over all partitions of A, i.e., all sets of $\{n_i\}$ which satisfy the constraint Eq. (1). For a collision involving ^{235}Ur+^{235}Ur, the number of possible fragmentations $p(A)$ is of order 10^{20}.

The partitioning of A also appears in permutation groups. In Ref. [14] a correspondence between clusters in a fragmentation process and cycles of the permutation group were established. One aspect of this paper is to explore this interrelationship between clusters, partitions, and cycles of the permutation group. Specifically, a cluster of j objects corresponds to a cycle of length j, and n_j is either the number of clusters or cycles of that size. The Π_A of Eq. (2) is then a classification of a permutation of A objects by its cycle class structure. The group is called symmetric group S_n, with $n=A$ here, and S_n has $A!$ elements. The $p(A)$ counts the total number of cycle classes. The number of permutations of A objects in a specific cycle class with n_1 unit cycles, n_2 cycles of length 2, etc., is given by Cauchy's number

$$M_2(A,\{n_j\})=\frac{A!}{\Pi_{j=1}^{A} j^{n_j}n_j!} \ . \tag{7}$$

The number of cycle classes $p(A)$ is also the number of irreducible representations of S_A [23]. The correspondence between the partitioning of an integer, cycles of a permutation, and fragmentation possibilities of an object is shown in Fig. 1.

A partition is sometimes specified by a decreasing set of numbers λ_i defined by the transformation

$$\begin{aligned}\lambda_1&=n_1+n_2+\cdots+n_A\ ,\\ \lambda_2&=n_2+\cdots+n_A\ ,\\ &\vdots\\ \lambda_A&=n_A\ .\end{aligned}\tag{8}$$

Here $A=\sum_i\lambda_i$ and $m=\lambda_1$. Note also $\lambda_1\geq\lambda_2\geq\lambda_3\geq\cdots$, and $n_1=\lambda_1-\lambda_2$, $n_2=\lambda_2-\lambda_3$, etc. For example, the division of 5 into 3+2 which is $\mathbf{n}=(2^1,3^1)=(0,1,1,0,0)_n$ in the n_i representation becomes $(2,2,1,0,0)_\lambda$ in the λ_i representation or $\boldsymbol{\lambda}=(2,2,1)_\lambda=(2^2,1)_\lambda$, where zeros are dropped. The partition 2+2+1 is represented by $\mathbf{n}=(2^2,1)$ in the $\mathbf{n}$ representation and by $\boldsymbol{\lambda}=(3,2)$ in the representation $\boldsymbol{\lambda}$. For each partition in the $\mathbf{n}$ representation, there is a partition with the same structure in the $\boldsymbol{\lambda}$ representation. As an example, for a given structure $(2^2,1)$, $\boldsymbol{\lambda}=(2^2,1)$ represents the partition of 3+2, and $\mathbf{n}=(2^2,1)$ represents the partition of 2+2+1. The $A=\sum_i\lambda_i$ can also be considered as the partition of an integer A into summands of smaller integers λ_i. For example, $\boldsymbol{\lambda}=(2^2,1)$ can be considered as a partition of 5 into $\sum_i\lambda_i=2+2+1$ and $\boldsymbol{\lambda}=(3,2)$ as 3+2. Thus, as we can see from Table I, the representation $\boldsymbol{\lambda}$ is conjugate to the representation $\mathbf{n}$.

The conjugate property between two representations $\mathbf{n}$ and $\boldsymbol{\lambda}$ can easily be visualized in terms of block diagram similar to a Ferrer diagram [17] or a Young tableau [23]. Here we can consider four types of diagrams. In Ferrer's block diagram, illustrated in Fig. 2(a), the partition $(n_1,n_2,\ldots,n_j,\ldots,n_A)=\mathbf{n}$ is represented by n_j rows of j horizontal blocks. They are placed in a diagram in descending order with the longest or largest j at the top. The Ferrer's diagram can also be viewed as a block diagram in $\boldsymbol{\lambda}=(\lambda_1,\lambda_2,\ldots,\lambda_A)$ space. Here λ_i blocks are put vertically in the ith column. The total number of rows (λ_1) is the multiplicity m and the area of this diagram (the total number of blocks) is A. A Young tableau in permutation groups is a similar type of diagram but, here, λ_i blocks are put horizontally in the ith row as shown in Fig. 2(b). We can obtain a Young tableau from Ferrer's block diagram by first turning the block diagram upside down and then by rotating it through 90° clockwise. This transformation between Ferrer's diagram and the Young tableau exhibits the conjugate relation between two representations of $\mathbf{n}$ and $\boldsymbol{\lambda}$. Table I also shows this conjugate relationship. Again, the total number of blocks is A and the number of columns (λ_1) is the multiplicity. A diagram constructed through the upside down version of a Ferrer's block diagram, Fig. 2(c), is useful in connecting a partition to the one-dimensional avalanche and sandpile slide models [4,5]. Avalanche models are generated by imposing a condition on block diagrams such as a constraint $n_k\leq\sigma$, where σ is a fixed number. Each slide is presented by a roll of a block to a lower column. With the constraint of $n_k\leq 1$, the number of partitions $q(A)$ of an integer A into integer summands without regards to order can be obtained through the generating function of Eq. (A5) in the Appendix. It is also useful to picture a nuclear fragmentation distribution

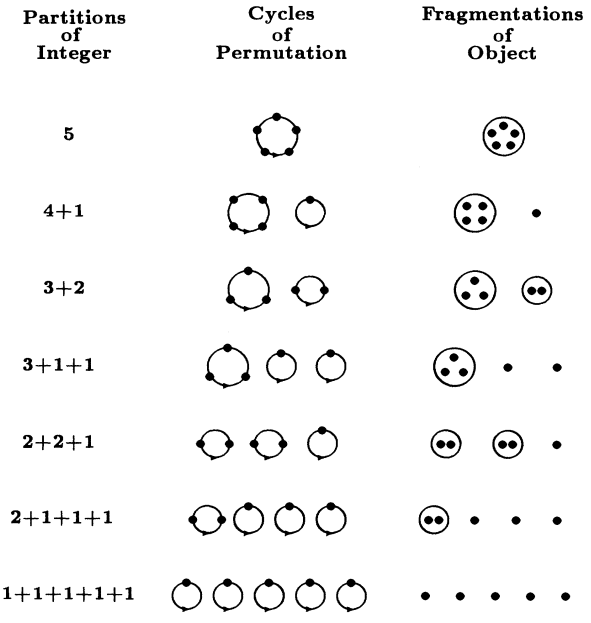

FIG. 1. Partitions of the integer 5, cycles of permutation group S_5, and the fragmentations of an object with five constituents. The solid circles represent the constituent elements. The large circle indicates the cyclic permutation of elements in the cycle and the constituents of the cluster are dots inside the circle in the fragmentation scheme.

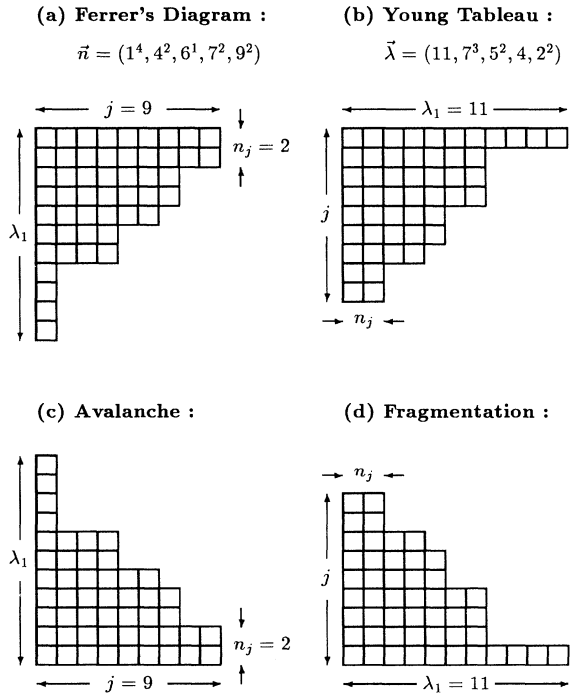

FIG. 2. Block diagrams for a partition Π_A of $A=50$ into $\mathbf{n}=(1^4,4^2,6^1,7^2,9^2)$ which is $\boldsymbol{\lambda}=(11,7^3,5^2,4,2^2)$.

in terms of a block representation with the cluster size j the vertical column and with the number of clusters of that size, the n_j, given horizontally. The columns are arranged in descending order from left to right as shown in Fig. 2(d). This fragmentation diagram is the horizontally reflected version of a Young tableau or the 90° counter clockwise rotation of a Ferrer's diagram. The multiplicity is just the number of columns. With this fragmentation diagram, a fragmentation process can be represented as the stepwise descent of blocks from a higher column to a lower one [14]. In these block diagrams, the $p(A)$ simply counts all possible arrangements of A blocks. Each arrangement of blocks is a unique partition represented as a staircase in Figs. 2(c) and 2(d). The $p(A,m)$ counts all possible arrangements with m fixed rows for a Ferrer's diagram or an avalanche diagram and with m fixed columns for a Young tableau or a fragmentation diagram.

III. CANONICAL PARTITION FUNCTIONS FOR FRAGMENTATION PHENOMENA AND CYCLE INDICATORS OF S_n

Consider an ensemble of partitions or cycle classes of A objects into smaller clusters or cycles which are weighted by x_j according to their size j. The weighted sum of all the partitions Π_A of A objects becomes the corresponding partition function. Let $W_A(\mathbf{n},\mathbf{x})$ be a weight function for a particular decomposition or partition $\mathbf{n}$. Here $\mathbf{x}=\{x_j\}=(x_1,x_2,\ldots,x_A)$ and $\mathbf{n}=\{n_j\}=(n_1,n_2,\ldots,n_A)$. The canonical partition function $Q_A(\mathbf{x})$ is given by

$$Q_A(\mathbf{x})=\sum_{\Pi_A} W_A(\mathbf{n},\mathbf{x}) . \tag{9}$$

When $W_A(\mathbf{n},\mathbf{x})$ is taken as

$$W_A(\mathbf{n},\mathbf{x})=M_2(A,\mathbf{n})\prod_{j=1}^{A} x_j^{n_j} , \tag{10}$$

with $M_2(A,\mathbf{n})$ given by Eq. (7), then $Q_A(\mathbf{x})$ is also the cycle indicator of the permutation of symmetric group S_A. In Refs. [14] and [15], a generating function for the canonical partition function was developed for fragmentation phenomena. Specifically, a generating function

$$Q(u,\mathbf{x})=\exp\left[\sum_{j=1}^{\infty} x_j\frac{u^j}{j}\right]=\sum_{A=0}^{\infty} Q_A(\mathbf{x})\frac{u^A}{A!} \tag{11}$$

was used to find the canonical partition function $Q_A(\mathbf{x})$ and the mean number of clusters of size k. A more general form for the grand canonical partition function $Q(u,\mathbf{x})$ is given and discussed in Ref. [16]. A physical meaning for $\mathbf{x}$ will be discussed for various physical systems in Sec. V.

When all the x_j in $\mathbf{x}$ are equal,

$$Q(u,x)=Q(u,\{x_j=x\})=(1-u)^{-x}$$

and

$$\begin{aligned} Q_A(x)=Q_A(\{x_j=x\})&=x(x+1)\cdots(x+A-1)\\ &=\frac{\Gamma(x+A)}{\Gamma(x)} . \end{aligned} \tag{12}$$

$\Gamma(x)$ is the gamma function. This canonical partition function $Q_A(x)$ has zeros at $x=0,-1,-2,\ldots,-(A-1)$ and the number increases with increasing A. When x is an integer, $x=n$, the $Q_A(n)=n(n+1)\cdots(n+A-1)$ can be written as a binomial or a negative binomial coefficient. In particular,

$$Q_A(n)=A!\begin{bmatrix} n+A-1 \\ A \end{bmatrix}=(-1)^A A!\begin{bmatrix} -n \\ A \end{bmatrix} , \tag{13}$$

where the binomial coefficient

$$\begin{bmatrix} n \\ A \end{bmatrix}$$

and the negative binomial coefficient

$$\begin{bmatrix} -n \\ A \end{bmatrix}$$

are

$$\begin{aligned} \begin{bmatrix} n \\ A \end{bmatrix}&=\frac{n(n-1)\cdots(n-A+1)}{A!}\\ &=\frac{\Gamma(n+1)}{\Gamma(n-A+1)\Gamma(A+1)} ,\\ \begin{bmatrix} -n \\ A \end{bmatrix}&=\frac{(-n)(-n-1)\cdots(-n-A+1)}{A!}\\ &=\frac{\Gamma(-n+1)}{\Gamma(-n-A+1)\Gamma(A+1)}\\ &=(-1)^A\begin{bmatrix} n+A-1 \\ A \end{bmatrix}\\ &=(-1)^A\frac{\Gamma(n+A)}{\Gamma(n)\Gamma(A+1)} . \end{aligned} \tag{14}$$

Here the binomial and the negative binomial are

$$\begin{aligned} (x_1+x_2)^n&=\sum_{A=0}^{n}\begin{bmatrix} n \\ A \end{bmatrix}x_1^A x_2^{n-A} ,\\ (x_1+x_2)^{-n}&=\sum_{A=0}^{\infty}\begin{bmatrix} -n \\ A \end{bmatrix}x_1^A x_2^{-(n+A)} , \end{aligned} \tag{15}$$

respectively. At $x=1$, $Q_A(1)=A!$.

$Q_A(x)$ is useful in studying permutations and fragmentations by the total number of cycles or multiplicity m with $m=\sum_j n_j=\lambda_1$. For example,

$$\begin{aligned} Q_5(x)&=x(x+1)(x+2)(x+3)(x+4)\\ &=24x^1+50x^2+35x^3+10x^4+x^5 \end{aligned}$$

and the coefficients in front of x^m, $m=1-5$, are signless Stirling numbers $(-1)^{A-m}S(A,m)$ of the first kind [18]. In general,

$$Q_A(x)=\frac{\Gamma(x+A)}{\Gamma(x)}=\sum_{m=1}^{A}(-1)^{A-m}S(A,m)x^m . \tag{16}$$

The sum of the coefficients (signless Stirling numbers) in $Q_A(x)$ is $Q_A(1)=A!$ which is $5!=120$ for $A=5$. The signless Stirling numbers appear in the theory of the multiplicity distribution developed in Ref. [14]. When each cycle is tagged with a different x_j, as in $Q_A(\mathbf{x})$, then

$$Q_5(\mathbf{x})=24x_5+30x_4x_1+20x_3x_2+20x_3x_1^2 +15x_2^2x_1+10x_2x_1^3+x_1^5 ,$$

where the subscript i in x_i corresponds to the length of the cycle or the size of the fragment and the power of x_i is n_i. The coefficients of each term are the Cauchy's number M_2 given by Eq. (7) (see Table I).

We next define a quantity $Q_A^m(\mathbf{x})$:

$$Q_A^m(\mathbf{x})=\sum_{\Pi_{A,m}} W_A(\mathbf{n},\mathbf{x}) , \tag{17}$$

where the sum is over all partitions Π_A of A with m fixed. Also, a quantity $Q_A^{n_k}(\mathbf{x})$ is defined by

$$Q_A^{n_k}(\mathbf{x})=\sum_{\Pi_{A,n_k}} W_A(\mathbf{n},\mathbf{x}) , \tag{18}$$

with the sum over all partitions Π_A of A with n_k specified. $Q_A^m(\mathbf{x})$ and $Q_A^{n_k}(\mathbf{x})$ are more constrained than $Q_A(\mathbf{x})$ and

$$Q_A(\mathbf{x})=\sum_{m=1}^{A} Q_A^m(\mathbf{x})=\sum_{n_k=0}^{A/k} Q_A^{n_k}(\mathbf{x}) . \tag{19}$$

For a system that has a total energy proportional to m, $Q_A^m(\mathbf{x})$ becomes a microcanonical partition function. Finally, define the pth order factorial [16] as

$$F_{A,p}^{n_k}(\mathbf{x})=n_k(n_k-1)(n_k-2)\cdots(n_k-p+1)Q_A^{n_k}(\mathbf{x}) =\left[\frac{x_k}{k}\right]^p\frac{A!}{(A-pk)!}Q_{A-pk}^{n_k-p}(\mathbf{x}) . \tag{20}$$

These quantities are used in describing the distribution of clusters as indicated in the following.

Once the canonical partition function $Q_A(\mathbf{x})$ is determined, the distribution of fragments in the canonical ensemble follows using general results obtained in Refs. [15] and [16]. Letting $\langle n_k\rangle$ be the mean number of clusters of size k,

$$\langle n_k\rangle=Y_A(k,\mathbf{x})=\frac{\sum_{n_k}F_{A,p=1}^{n_k}(\mathbf{x})}{Q_A(\mathbf{x})} =\left[\frac{x_k}{k}\right]\frac{A!}{(A-k)!}\frac{Q_{A-k}(\mathbf{x})}{Q_A(\mathbf{x})} . \tag{21}$$

The contribution of partitions with fixed multiplicity m to the mean cluster distribution $\langle n_k\rangle$ of size k is simply

$$\langle n_k\rangle_m=\left[\frac{x_k}{k}\right]\frac{A!}{(A-k)!}\frac{Q_{A-k}^{m-1}(\mathbf{x})}{Q_A(\mathbf{x})} . \tag{22}$$

The total yield of clusters of size k is then made from a sum of contributions from each multiplicity m

$$\langle n_k\rangle=\sum_{m=1}^{A}\langle n_k\rangle_m . \tag{23}$$

When the denominator $Q_A(\mathbf{x})$ in Eq. (22) is replaced by the microcanonical partition function $Q_A^m(\mathbf{x})$, the resulting mean cluster size distribution of Eq. (22) is that arising from a microcanonical ensemble with fixed multiplicity m and A [16].

Correlations and moments are also easily obtained from $Q_A(\mathbf{x})$. The correlation $\langle n_kn_j\rangle$ for $k\neq j$ is given by

$$\langle n_kn_j\rangle=\left[\frac{x_k}{k}\frac{x_j}{j}\right]\frac{A!}{(A-k-j)!}\frac{Q_{A-k-j}(\mathbf{x})}{Q_A(\mathbf{x})} , \tag{24}$$

while the second factorial moment is

$$\langle n_k(n_k-1)\rangle=\frac{\sum_{n_k}F_{A,p=2}^{n_k}(\mathbf{x})}{Q_A(\mathbf{x})} =\left[\frac{x_k}{k}\right]^2\frac{A!}{(A-2k)!}\frac{Q_{A-2k}(\mathbf{x})}{Q_A(\mathbf{x})} . \tag{25}$$

In fact, defining $\tilde{n}_k^p=n_k(n_k-1)\cdots(n_k-p+1)$, the factorial moment of order p is given by

$$\langle\tilde{n}_k^p\rangle=\frac{\sum_{n_k}F_{A,p}^{n_k}(\mathbf{x})}{Q_A(\mathbf{x})} =\left[\frac{x_k}{k}\right]^p\frac{A!}{(A-pk)!}\frac{Q_{A-pk}(\mathbf{x})}{Q_A(\mathbf{x})} . \tag{26}$$

Also, for $k\neq j$,

$$\langle\tilde{n}_k^p\tilde{n}_j^l\rangle=\left[\frac{x_k}{k}\right]^p\left[\frac{x_j}{j}\right]^l\frac{A!}{(A-pk-lj)!} \times\frac{Q_{A-pk-lj}(\mathbf{x})}{Q_A(\mathbf{x})} . \tag{27}$$

The above results are easily generalized to three and more sizes, i.e.,

$$\langle n_kn_jn_l\cdots\rangle=\left[\frac{x_k}{k}\frac{x_j}{j}\frac{x_l}{l}\cdots\right]\frac{A!}{[A-(k+j+l+\cdots)]!} \times\frac{Q_{A-[k+j+l+\cdots]}(\mathbf{x})}{Q_A(\mathbf{x})} , \tag{28}$$

where $k,j,l,\ldots,$ are all different from each other. From the factorial moment of Eq. (26), we can find the usual moment $\langle n_k^p\rangle$. We next turn our attention to a determination of the partition functions $Q_A(\mathbf{x})$ for the various exactly soluble cases.

IV. VARIOUS EXACTLY SOLUBLE MODELS

The previous section summarizes general expressions for properties associated with cluster sizes arising from fragmentation phenomena and related partitioning problems. Once the partition function $Q_A(\mathbf{x})$ is evaluated, the expressions given in Sec. III can be used to obtain the desired quantities. This section gives some special cases which are exactly soluble. Various models for the canonical ensemble partition function $Q_A(\mathbf{x})$ are discussed. The various models show a rich variety of different possibilities and behaviors. They will be related to various

areas such as nuclear physics, astrophysics, population genetics, and social behavior in Sec. V.

A. Model based on a single tuning parameter x: Length scales and scale invariance

When all the x_j's are equal to x, then the canonical partition function becomes $Q_A(x)=x(x+1)\cdots(x+A-1)$ as given by Eq. (12). Thus, using Eqs. (21)–(25),

$$\langle n_k\rangle=\left[\frac{x}{k}\right]\frac{A!}{(A-k)!}\frac{\Gamma(x+A-k)}{\Gamma(x+A)}\ ,$$

$$\langle n_k(n_k-1)\rangle=\left[\frac{x}{k}\right]^2\frac{A!}{(A-2k)!}\frac{\Gamma(x+A-2k)}{\Gamma(x+A)}\ , \tag{29}$$

$$\langle n_k n_j\rangle=\left[\frac{x}{k}\right]\left[\frac{x}{j}\right]\frac{A!}{(A-k-j)!}\frac{\Gamma(x+A-k-j)}{\Gamma(x+A)}\ .$$

Properties of the distribution of cluster sizes were discussed in detail in Refs. [14] and [15]. Moreover, a thermodynamic model for x was developed [14,16]. A comparison between the population genetics model [24,25] and the x model of fragmentation is developed in Ref. [26]. The physical contents of parameter x is discussed in Sec. V.

We note the following features of the x model. At $x=0$, only one cluster of size A exists; we called it the fused mode. At $x=\infty$, only A monomers exist, i.e., total fragmentation (vaporization) mode. These two extreme cases have zero fluctuations. At $x=1$,

$$\langle n_k\rangle=\frac{1}{k}\ ,$$

$$\langle n_k n_j\rangle=\left[\frac{1}{k}\right]\left[\frac{1}{j}\right]=\langle n_k\rangle\langle n_j\rangle\ , \tag{30}$$

$$\langle n_k(n_k-1)\rangle=\frac{1}{k^2}=\langle n_k\rangle^2\ ,$$

for $k\le A$, $k+j\le A$, and $2k\le A$, respectively. Otherwise, the quantities in Eq. (30) are zero. The last result of Eq. (30) shows that the fluctuation is the same as the mean number of clusters for $2k\le A$, i.e.,

$$\langle n_k^2\rangle-\langle n_k\rangle^2=\langle n_k\rangle=\frac{1}{k}\ . \tag{31}$$

The results of Eqs. (30) and (31) are independent of the size A so long as the constraints are satisfied. When x is an integer $x=n$, we have

$$\langle n_k\rangle=\left[\frac{n}{k}\right]\frac{(A-k+1)(A-k+2)\cdots(A-k+n-1)}{(A+1)(A+2)\cdots(A+n-1)}\ . \tag{32}$$

This result shows that $\langle n_k\rangle$ depends on the size A except at the point $x=n=1$. Equation (32) can also be rewritten as

$$\langle n_k\rangle=\left[\frac{n}{k}\right]\left[\begin{matrix}n+A-k-1\\A-k\end{matrix}\right]\Big/\left[\begin{matrix}n+A-1\\A\end{matrix}\right]$$

$$=(-1)^k\left[\frac{n}{k}\right]\left[\begin{matrix}-n\\A-k\end{matrix}\right]\Big/\left[\begin{matrix}-n\\A\end{matrix}\right]\ , \tag{33}$$

and, thus, in terms of the binomial or negative binomial coefficient given by Eq. (14). Here x ranges from zero to infinity. A simple transformation to a variable $t=1/(1+x)$ changes the domain of x to the interval from 0 to 1: $x=0$ to $t=1$, $x=\infty$ to $t=0$, and $x=1$ to $t=\frac{1}{2}$.

As already noted, the cluster size distribution at $x=1$ is $\langle n_k\rangle=1/k$ and is thus scale invariant (i.e., independent of A) except for the trivial constraint $k<A$. A distribution having a length scale of length K is characterized by

$$\langle n_k\rangle\propto e^{-k/K}\ . \tag{34}$$

To obtain a scale invariant behavior such as $1/k$ from Eq. (34), a distribution of length scales must be present as can be seen from

$$\frac{\Gamma(n+1)}{k^{n+1}}=\int_0^\infty\frac{dK}{K^{n+2}}e^{-k/K}\ . \tag{35}$$

Thus, the hyperbolic behavior $1/k$ can be thought of as arising in a system in which all length scales K are present with a density $1/K^2$. This result is well known in $1/f$ noise where a similar discussion is given for the origin of this noise [11]. Moreover, since $\langle n_k^2\rangle-\langle n_k\rangle^2=\langle n_k\rangle=1/k$, the fluctuation has all length scales present in $\langle n_k\rangle$ at $x=1$. When $x\gg A$, the behavior of $\langle n_k\rangle$ for large k [14] is

$$\langle n_k\rangle\approx\frac{A}{k}e^{-(k-1)\ln(x/A)}\approx e^{-k\ln(x/A)}\ , \tag{36}$$

so that a length scale is $K=1/\ln(x/A)$. Scale invariance also appears in sandpile and avalanche theories [4,5] and in other power-law behaviors.

Before ending, we note that the scale invariant distribution $\langle n_k\rangle=1/k$ can be rewritten as a distribution of frequency sizes. A given cycle of length k is cyclic with period k. The length 3 permutation

$$a=\begin{bmatrix}1&2&3\\2&3&1\end{bmatrix}$$

is such that $a^3=e$, the identity element. Note that a frequency can be associated with a period k such that $kf_k=1$, and thus $f_k=1/k$. In nuclear physics, the harmonic-oscillator frequency f_k associated with a nucleus of size k (having k nucleons) is given by $hf_k=\hbar\omega_k=a/k^{1/3}$, where $a\approx 40$ MeV for k large. Using the transformation of $n(f)=\langle n_k\rangle dk/df$, we obtain $n(f)\sim 1/f$ when $\langle n_k\rangle=1/k$ for the permutation cycle and the nuclear harmonic oscillator.

B. Sum rules, cumulative mass, moments, and correlations

This section considers the gross features of the distribution $\langle n_k \rangle$ of cluster sizes by considering sum rules and moments of this distribution. The moments are obtained by multiplying each $\langle n_k \rangle$ by some power of k and summing over k. The zeroth and the first moments are the mean multiplicity and the total number of elements A, respectively,

$$\sum_{k=1}^{A} \langle n_k \rangle = \langle m \rangle \ , \qquad \sum_{k=1}^{A} k \langle n_k \rangle = A \ . \tag{37}$$

The first moment result follows from the conservation constraint $\sum_k k n_k = A$. The results of Eq. (37) are true for arbitrary x_j's and not just for the $x_j = x$ case.

Another quantity of interest is the cumulative mass $M(s)$,

$$M(s) = \sum_{k=1}^{[s]+1} k \langle n_k \rangle \ , \tag{38}$$

where the $[s]$ is the greatest integer in the continuous real value s, i.e., $[s] \le s < [s]+1$. Due to the sum rule Eq. (37), the cumulative mass becomes A for $s \ge A-1$, i.e., $M(s \ge A-1) = A$. For the $x_j = x = 1$ case, this cumulative mass $M(s)$ becomes a uniform staircase in which the step size is independent of the position k and the size A of the staircase. This result is shown in Fig. 3(a). For $x = n > 1$, the cumulative mass $M(s)$ is no longer a uniform staircase as can be seen from Eq. (32), i.e., the step size depends on k and A [see Fig. 3(a) for $x = 3$]. For x_j chosen such that $x_j = 0$ for some specific j's and x for others, intermissions or breaks appear in $M(s)$ of Eq. (38). An extreme example in a continuum model is a Devil's staircase obtained by Cantor's rule [14].

Using Eq. (48) in the next subsection, we can obtain all higher-order moments for the $x_i = x$ case. Specifically, the second, the third, and the fourth moments are

$$\sum_{k=1}^{A} k^2 \langle n_k \rangle = \frac{A(A+x)}{(x+1)} \ , \qquad \sum_{k=1}^{A} k^3 \langle n_k \rangle = \frac{A(A+x)(2A+x)}{(x+1)(x+2)} \ , \qquad \sum_{k=1}^{A} k^4 \langle n_k \rangle = \frac{A(A+x)[6A(A+x)+x(x-1)]}{(x+1)(x+2)(x+3)} \ . \tag{39}$$

At $x = 1$ [14], the second moment is a statement that the sum of the first A integers is $A(A+1)/2$, while the third moment is the result that the sum of the squares of the first A integers is $A(A+1)(2A+1)/6$ and the fourth is the sum of cubic integers, which is $A^2(A+1)^2/4$. Moments of a size distribution have been used in Ref. [27] to study the energy dependence of critical exponent of mass distributions in nuclear multifragmentation.

Using the notation $Y_A(k,\mathbf{x})$ of Eq. (21), Eq. (24) can be rewritten as

$$\langle n_k n_j \rangle = Y_A(k,\mathbf{x}) Y_{A-k}(j,\mathbf{x}) = Y_{A-j}(k,\mathbf{x}) Y_A(j,\mathbf{x}) \ .$$

$\langle n_k n_j \rangle = 0$ for $k+j > A$. Then we obtain the following result for correlations in cluster sizes:

$$\sum_{k=1}^{A} \sum_{j=1}^{A} k^m j^l \langle n_k n_j \rangle = \sum_{k=1}^{A} k^m Y_A(k,\mathbf{x}) \sum_{j=1}^{A-k} j^l Y_{A-k}(j,\mathbf{x}) \ . \tag{40}$$

Specifically, using Eq. (37) for arbitrary x_j's, we have

$$\begin{aligned} \sum_{k=1}^{A} \sum_{j=1}^{A} kj \langle n_k n_j \rangle &= \sum_{k=1}^{A} k Y_A(k,\mathbf{x}) \sum_{j=1}^{A-k} j Y_{A-k}(j,\mathbf{x}) \\ &= \sum_{k=1}^{A} \langle n_k \rangle k(A-k) \\ &= A^2 - \sum_{k=1}^{A} k^2 \langle n_k \rangle \ . \end{aligned} \tag{41}$$

When $x_i = x$ for all i and using Eq. (39), the following results are obtained:

$$\sum_{k=1}^{A} \sum_{j=1}^{A} kj \langle n_k n_j \rangle = \frac{xA(A-1)}{(x+1)} \ , \tag{42}$$

$$\sum_{k=1}^{A} \sum_{j=1}^{A} k^2 j^2 \langle n_k n_j \rangle = \frac{xA(A+x)[A(A+x)-(x+1)]}{(x+1)(x+2)(x+3)} \ .$$

Similar types of correlations have been used in Ref. [28] to study critical behavior in nuclear multifragmentation. For the case of $x = 1$, the results of Eq. (42) reduce to $A(A-1)/2$ and $(A+2)(A+1)A(A-1)/24$.

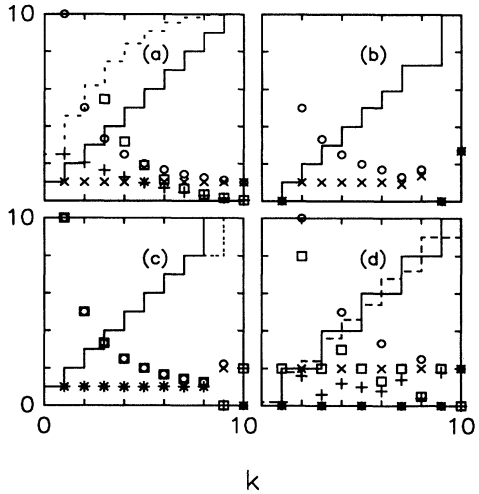

FIG. 3. Staircases $M(s)$ (solid and dashed lines), cluster distributions $A\langle n_k \rangle$ (circles and squares), and probabilities $P_A(k,\mathbf{x})$ (cross and plus) for various models with $A = 10$: (a) One-variable x model of Sec. IV A with $x = 1$ (solid line, circle, and cross) and with $x = 3$ (dashed line, square, plus); (b) two-variable x-y model of Sec. IV D with $x = 1$ and $y = 0$; (c) even (solid line, circle, cross) and odd (dashed line, square, plus) permutations of Sec. IV E with $x = 1$; (d) the case of $x_k = 1/(1-q^k)$ of Sec. IV G with $q = -1$ for $A = 10$ (solid line, circle, cross) and for $A = 9$ (dashed line, square, plus).

C. Fragmentation and probability theory

Since the sum rule for the first moment Eq. (37), which is the total number conservation Eq. (1), is independent of the parameter x_j's, we can define a probability distribution $P_A(k,\mathbf{x})$ as

$$P_A(k,\mathbf{x})=\frac{k\langle n_k\rangle}{A} . \tag{43}$$

$P_A(k,\mathbf{x})$ is the fraction of the total mass in clusters of size k and is thus the probability of a particle belonging to clusters of size k. $P_A(k,\mathbf{x})$ also represents the ratio of the step height of a staircase Eq. (38) to the total height A (see Fig. 3) at the kth step. $AP_A(k,\mathbf{x})$, in a continuum limit for k, corresponds to the slope of the cumulative mass $M(s)$. The probability of Eq. (43) is developed and related with various probability theories in Ref. [29] for the $x_j=x$ case. With the probability distribution of Eq. (43), $\sum_k P_A(k,\mathbf{x})=1$ and the $(l+1)$th-order moment of $\langle n_k\rangle$ becomes the average of the lth moment $\langle k^l\rangle$ of $P_A(k,\mathbf{x})$ times A:

$$\langle k^l\rangle=\sum_{k=1}^{A} k^l P_A(k,\mathbf{x})=\frac{1}{A}\sum_{k=1}^{A} k^{l+1}\langle n_k\rangle . \tag{44}$$

Specifically, the second, third, and fourth moments of Eq. (39) are $A\langle k\rangle$, $A\langle k^2\rangle$, and $A\langle k^3\rangle$, respectively, when $x_i=x$.

When all the x_j's are x, $P_A(k,\mathbf{x})$ is

$$P_A(k,x)=x\begin{bmatrix}A-1\\k-1\end{bmatrix}B(x+A-k,k) . \tag{45}$$

Here,

$$\begin{bmatrix}A-1\\k-1\end{bmatrix}$$

is the binomial coefficient given by Eq. (14) and $B(x+A-k,k)$ is a beta function given by

$$B(a,b)=\frac{\Gamma(a)\Gamma(b)}{\Gamma(a+b)}=\int_0^1 dp\, p^{a-1}(1-p)^{b-1} . \tag{46}$$

Since

$$k(k+1)\cdots(k+n-1)B(x+A-k,k)=(x+A)(x+A+1)\cdots(x+A+n-1)B(x+A-k,k+n) , \tag{47}$$

the factorial moments in $P_A(k,x)$ are given by

$$\begin{aligned}\langle k(k+1)(k+2)\cdots(k+n-1)\rangle&=\sum_{k=1}^{A} k(k+1)(k+2)\cdots(k+n-1)P_A(k,x)\\&=n!\frac{\Gamma(x+1)}{\Gamma(x+1+n)}\frac{\Gamma(x+A+n)}{\Gamma(x+A)} .\end{aligned} \tag{48}$$

Here we have used the integral representation of the β function. From Eq. (48) or (39), the average of $\langle k\rangle$ and its fluctuation Δk become

$$\begin{aligned}\langle k\rangle&=\sum_{k=1}^{A} kP_A(k,x)=\frac{(A+x)}{(x+1)} ,\\ \langle k^2\rangle&=\sum_{k=1}^{A} k^2P_A(k,x)=\frac{(A+x)(2A+x)}{(x+1)(x+2)} ,\\ \Delta k&=\langle k^2\rangle-\langle k\rangle^2=\frac{(A+x)(A-1)x}{(x+1)^2(x+2)} .\end{aligned} \tag{49}$$

The average of $\langle k\rangle$ is A for $x=0$ and 1 for $x=\infty$ with zero fluctuation ($\Delta k=0$) for both of these cases. When $x=1$, the average of $\langle k\rangle$ becomes $(A+1)/2$ with its fluctuation $\Delta k=(A^2-1)/12$.

Using the integral representation of Eq. (46) for the β function, $P_A(k,x)$ can be rewritten as

$$P_A(k,x)=\int_0^1 dp\frac{(A-1)!}{(A-k)!(k-1)!}p^{k-1}(1-p)^{A-k}u(x,p) , \tag{50}$$

where

$$u(x,p)=x(1-p)^{x-1} . \tag{51}$$

$\int_0^1 u(x,p)dp=1$. Thus, $u(x,p)$ can be considered as a density function weighting each point in p space, that is, the probability p of a binomial distribution. This expression for $P_A(k,x)$ is a special case of a randomized Bernoulli distribution [30] where the probability of success p for a trial is treated as a random variable with a density $u(x,p)$. The number of successes out of $A-1$ trials becomes $s=k-1$. The density function $u(x,p)$ has the following simple properties: $u(x=1,p)=1$ which is a uniform distribution giving $P_A(k,x=1)=1/A$ from Eqs. (46) and (50); $\lim_{x\to 0}u(x,p)=\delta(1-p)$ which has a probability of success equal to unity and $P_A(k,x=0)=\delta_{k,A}$; $\lim_{x\to\infty}u(x,p)=\delta(p-0)$ so that the probability of success is zero giving $P_A(k,x=\infty)=\delta_{k,1}$.

Using Eq. (43), we can also relate the fragment distribution $\langle n_k\rangle$ to the probability $P_A(k,\mathbf{x})$ of $k-1$ successes (heads) out of $A-1$ trials (throws) of a skewed coin [$u(\mathbf{x},p)$]. $\langle n_k\rangle$ can also be related to the probability that a face with k dots of a lopsided die with A faces touches the table. Here the size k of a cluster corresponds to the number of dots on a face. The total number of elements A is the number of faces of a die. The probability $P_A(k,\mathbf{x})$ that the ith nucleon belongs to one of the clusters of size k corresponds to the probability that the face with k dots touches the table on the ith throw of the total A throws of a die with A faces. The

extra factor $u(x,p)$ of Eq. (51) determines the skewness of a coin or the lopsidedness of a die. Inversely, if we know a probability $P_A(k,\mathbf{x})$, then the distribution of clusters is $\langle n_k \rangle = (A/k)P_A(k,\mathbf{x})$ through Eq. (43)

If $u(x,p)$ in Eq. (50) had been a δ function at p_0, such as $u(x,p)=\delta[p-p_0(x)]$, then

$$P_A(k,p_0)=\begin{bmatrix} A-1 \\ k-1 \end{bmatrix} p_0^{k-1}(1-p_0)^{A-k} , \tag{52}$$

which is a binomial distribution with probability $p_0(x)$. This is the probability of having $k-1$ heads in the $A-1$ tosses of a two-sided coin which is skewed with probability p_0 of heads. With this probability, the mean cluster size $\langle k \rangle$ and its fluctuation are

$$\begin{aligned} \langle k \rangle &= \sum_{k=1}^{A} kP_A(k,p_0)=(A-1)p_0+1 , \\ \Delta k &= (A-1)p_0(1-p_0) . \end{aligned} \tag{53}$$

For this case, we have

$$\langle n_k \rangle = \frac{A!}{(A-k)!k!}[p_0(x)]^{k-1}[1-p_0(x)]^{A-k} , \tag{54}$$

and thus a scale invariant distribution does not exist. The probability of Eq. (52) is also the same as the Rowlinson urn [31,32] containing two colored balls with a fraction p_0 of one color and a fraction $1-p_0$ of another color.

D. Models with two tuning parameters: Situations without monomers

In our next level of complexity, we take $x_k = xy^{\delta_{k,1}}$; that is, $\mathbf{x}=(xy,x,x,\ldots,x)$. Even though only a single term in the set of $\{x_i\}$ is treated differently, the expressions are much more complex than the previous case with one parameter. In this x-y model, the monomer is put on a different footing because it may behave quite differently. For example, quarks and antiquarks are always bound into clusters of size two or more to form color singlets (hadrons). This situation excludes the existence of monomers and this physical situation corresponds to setting $y=0$. Here the objects are taken to be one type and we hope to generalize the model to more complex situations in the future. For the symmetry group S_n, the case $y=0$ corresponds to the subclass of permutations with no unit cycles. A monomer is also quite different because of its lack of binding and internal excitations. An application of the x-y model to nuclear fragmentation can be found in Ref. [16]. An illustration of the results of this section to astrophysics and social behavior will be given in Sec. V along with other models developed later.

The exponential generating function of Eq. (11) for $Q_A(\mathbf{x})$ is now

$$\begin{aligned} Q(u,\mathbf{x})=Q(u,x,y) &= \exp\left[xyu+\frac{xu^2}{2}+\frac{xu^3}{3}+\cdots\right] \\ &= \frac{1}{(1-u)^x}e^{x(y-1)u} , \end{aligned} \tag{55}$$

where $\mathbf{x}=(xy,x,x,\ldots)$. From $Q(u,\mathbf{x})$, one can obtain the canonical partition function $Q_A(x,y)$ for this model as

$$Q_A(x,y)=\sum_{r=0}^{A}\frac{A!}{r!(A-r)!}\frac{\Gamma(x+r)}{\Gamma(x)}[x(y-1)]^{A-r} . \tag{56}$$

When $y=1$,

$$Q_A(x,y=1)=Q_A(x)=x(x-1)\cdots(x+A-1) .$$

Having obtained $Q_A(x,y)$, $\langle n_k \rangle$ follows Eq. (21):

$$\langle n_k \rangle = \frac{xy^{\delta_{k,1}}}{k}\frac{A!}{(A-k)!}\frac{Q_{A-k}(x,y)}{Q_A(x,y)} .$$

Also, the correlations and fluctuations follow from Eqs. (24)–(28). At $x=1$ and $y=1$, $\langle n_k \rangle = 1/k$, which is a power-law behavior. Further details are studied in Ref. [15] with general y values; here we will study the $y=0$ case in more detail.

As mentioned above, when $y=0$, no monomer exists. We call $Q_A(x,y=0)=D_A(x)$, which can be rewritten as

$$D_A(x)=\sum_{j=0}^{A}\begin{bmatrix} A \\ j \end{bmatrix}(-x)^j Q_{A-j}(x) \tag{57}$$

from Eq. (56) and is generated by

$$Q(u,x,y=0)=\frac{1}{(1-u)^x}e^{-xu}=\sum_{A=0}^{\infty}D_A(x)\frac{u^A}{A!} . \tag{58}$$

$Q_{A-j}(x)$ is given by Eq. (12) or (16) and $Q_0(x)=1$. Expanding $D_A(x)$ in powers of x, we have

$$\begin{aligned} D_A(x) &= \sum_{m=1}^{A} D(A,m)x^m , \\ D(A,m) &= \sum_{j=0}^{A}\begin{bmatrix} A \\ j \end{bmatrix}(-1)^{A-m+j}S(A-j,m-j) , \end{aligned} \tag{59}$$

where $S(A-j,m-j)$ is a Stirling number of the first kind and $D(A,m)$ is called an associated Stirling number of the first kind. This associated number is obtained by summing the Cauchy number $M_2(A,\mathbf{n})$ of Eq. (7) over all partitions of A with fixed multiplicity m and with $n_1=0$. $D_A(x)$ satisfy a recurrence relationship [17]

$$D_{A+1}(x)=AD_A(x)+AxD_{A-1}(x) \tag{60}$$

with $D_0(x)=1$ and $D_1(x)=0$. For example, $D_2(x)=x$, $D_3(x)=2x$, $D_4(x)=3x^2+6x$, and $D_5(x)=20x^2+24x$.

For $y=0$, $\langle n_k \rangle = 0$ for $k=1$ and $k=A-1$. For all other k,

$$\langle n_k \rangle \approx \frac{xA}{k(A-k)} \tag{61}$$

for $x \ll 1$ and $y=0$. The mean number of clusters at $x=1$ and $y=0$ is

$$\langle n_k \rangle = \frac{1}{k}\frac{A!}{(A-k)!}\frac{D_{A-k}}{D_A}=\frac{1}{k}\frac{\sum_{j=0}^{A-k}(-1)^j/j!}{\sum_{j=0}^{A}(-1)^j/j!} , \tag{62}$$

except for $k=1$ and $A-1$ which do not exist at $y=0$. From Eq. (56) or (57), D_n is given by

$$D_n = D_n(x=1) = n! \sum_{j=0}^{n} \frac{(-1)^j}{j!} \tag{63}$$

and is called the number of derangements. From the result of Eq. (63), it is easy to show that D_n satisfy a recurrence relationship

$$D_n = nD_{n-1} + (-1)^n .$$

This relation is very similar to the recurrence relationship for factorials; the result differs from it because of the second term $(-1)^n$. D_n appears in card shuffling and matching questions [17] and counts the number of permutations in which no card is in its original position once the deck is shuffled. This problem is known as "*le problème de rencontres.*" $\mathcal{P}_A = D_A/A!$ is then the probability that no card will be in its original position after shuffling. Thus, the mean total mass in clusters of size k, $k\langle n_k \rangle$, is the ratio of two such probabilities, consisting of a deck of cards of size $A-k$ and a deck of cards of size A [see Eq. (62)]. When n in D_n is large, then

$$D_n \approx n! \frac{1}{e} . \tag{64}$$

Thus, for small k and large A, $\mathcal{P}_A \approx 1/e$ and $\langle n_k \rangle \approx 1/k$ for $x=1$ and $y=0$. However, Eq. (62) is not a perfect power law in k for all k. Figure 3(b) shows the cumulative mass $M(s)$ for this case.

Through the relation of Eq. (43), we can relate a fragmentation process without monomers to a dice problem. At $y=0$ and $x=1$, the probability $P_A(k,\mathbf{x}) = k\langle n_k \rangle / A$ is

$$P_A(k, x=1, y=0) = \frac{1}{A} \frac{\sum_{j=1}^{A-k} (-1)^j/j!}{\sum_{j=1}^{A} (-1)^j/j!} \tag{65}$$

except for $k=1$ and $A-1$ which do not exist, i.e., $P_A(k=1,x=1,y=0)=0$ and $P_A(k=A-1,x=1,y=0)=0$. Thus, this special case of the fragmentation of A objects without monomers is the same as rolling a die with $A-2$ faces. On the die, there is no face with either $k=1$ or $A-1$ dots. Equation (65) fixes the probability of each face of a lopsided die.

Before ending, we note that the generating function for cases when a certain fragment size (say l) is treated with different weight given by $x_l = xy$ is

$$Q(u,\mathbf{x}) = \frac{1}{(1-u)^x} e^{(y-1)xu^l/l} . \tag{66}$$

Then the corresponding canonical partition function $Q_A(\mathbf{x})$ follows through Eq. (11). The case without monomers discussed above has $l=1$ and $y=0$.

E. Separation by even and odd permutations: The appearance of a jump at the end of a uniform staircase

This section also looks into the question of what happens to the distribution of clusters if we are limited to a subset of partitions which is a fraction of the complete set. The $y=0$ or no monomer situation discussed in the previous section also considered a subset of all partitions. The subsets that will be taken here are either the even or odd permutations. A permutation is even if it contains an even number of transpositions and odd if it contains an odd number of transpositions. A cycle of even length is odd and one of odd length is even. The cycle indicators of even or odd permutations, Q_A^+ or Q_A^-, respectively, are

$$Q_A^{\pm}(\mathbf{x}) = \tfrac{1}{2}[Q_A(x_1,x_2,x_3,x_4,\ldots,x_A) \pm Q_A(x_1,-x_2,x_3,-x_4,\ldots,(-1)^{A+1}x_A)] . \tag{67}$$

The parity, which is plus for even and minus for odd permutations, is determined by the number of even cycles; specifically, the parity is $(-1)^{n_2+n_4+n_6+\cdots}$. Due to Eqs. (1) and (3), the parity of a given multiplicity m for a given A is $(-1)^{A+m}$. Thus, states of the same multiplicity, even though they contain different classes, have the same parity (see Table I).

The even permutations form a group [23], the alternating group A_n containing $n!/2$ elements ($n>1$). In fact, the alternating group A_n is the only invariant subgroup of the symmetric group S_n for $n>4$. The quotient group or factor group S_n/A_n has two one-dimensional representations, one being the identity or symmetric representation and the other the antisymmetric representation with characters $+1$ for even and -1 for odd permutations.

Models based on this distinction between even and odd cycles are easily solved. We consider the case $x_j = x$ for all j. Since

$$Q(u,\{x_j=(-1)^{j+1}x\}) = (1+u)^x ,$$

we obtain

$$Q_A^{\pm}(x) = \tfrac{1}{2}[Q_A(x^+) \pm Q_A(x^-)] . \tag{68}$$

$Q_A(x^+) = Q_A(x)$ of Eq. (12), which is the partition for $\mathbf{x}=\{x_j=x\}$ and

$$Q_A(x^-) = x(x-1)\cdots(x-A+1) = \sum_{m=0}^{A} S(A,m)x^m , \tag{69}$$

which is for $\mathbf{x}=\{x_j=(-1)^{j+1}x\}$. All properties of the cluster sizes are determined by the results of Sec. III. However, due to different sets of x_j's in $Q_A(x^+)$ and in $Q_A(x^-)$, we should use the proper x_k's in the corresponding $Q_A(x^{\pm})$ in Eqs. (20)–(28). Notice here that $Q_A(x^-)$ has zeros at $x=0,1,2,\ldots,A-1$, which are positive integers in contrast to $Q_A(x^+)$ of Eq. (12), which has zeros at negative integers. If we consider the $Q_A(x^-)$ piece only, then the mean cluster distribution $\langle n_k \rangle$ in the ensemble of $Q_A(x^-)$ becomes negative for some k depending on the value of x which is nonphysical.

Here we look at the mean number $\langle n_k \rangle^{\pm}$ of clusters of size k in the ensemble of even or odd permutations $Q_A^{\pm}(x)$:

$$\langle n_k \rangle^{\pm} = \frac{A!}{(A-k)!} \frac{(1/2)\{(x/k)Q_{A-k}(x^+) \pm [(-1)^{k+1}x/k]Q_{A-k}(x^-)\}}{Q_A^{\pm}(x)} . \tag{70}$$

For integer $x=n<A$, $Q_A(x^-)=0$ and thus $Q_A^{\pm}(x)=Q_A(x)$ for $A \geq (n+1)$. Thus, when $x=n$, all properties for clusters of size $k<(A-n)$ are the same as the $Q_A(x)$ case considered in Sec. IV A. For example, at $x=1$, Eq. (70) becomes $\langle n_k \rangle^{\pm}=1/k$ for $k=1$ to $A-2$, while, for $k=A-1$ and $k=A$,

$$\langle n_{A-1} \rangle^{\pm} = \frac{1 \pm (-1)^A}{A-1} ,$$
$$\langle n_A \rangle^{\pm} = \frac{1 \pm (-1)^{A+1}}{A} . \tag{71}$$

Thus, the distributions $\langle n_k \rangle^{\pm}$ fall exactly as a hyperbolic power law from $k=1$ to $A-2$ and a break appears at either $k=A-1$ or $k=A$ [see Fig. 3(c)]. For even A, $\langle n_A \rangle^{+}=0$ and $\langle n_A \rangle^{-}=2/A$, and for odd A, $\langle n_A \rangle^{+}=2/A$ and $\langle n_A \rangle^{-}=0$. Also, the $k=A-1$ cluster is not present in even permutations ($\langle n_{A-1} \rangle^{+}=0$) for A odd and is not present in odd permutations ($\langle n_{A-1} \rangle^{-}=0$) for even A. The results of Eq. (71) can be understood as follows. Only one cluster of size A can exist alone ($A=A$) and only one cluster of size $A-1$ can exist together with only one monomer [$A=(A-1)+1$]. For A even, a cycle of length A is odd; thus, the cluster of size A exists only in odd permutation for even A. The cycle of length $A-1$ is even for A even and is odd for odd A. However, the unit cycle is always even. Thus, a partition into one cluster of size $A-1$ together with one monomer becomes even for even A and odd for odd A. The more remarkable feature is that a hyperbolic power law is maintained until the last two k's, $k=A-1$ and $k=A$ [see Fig. 3(c)]. These results show that the power law is exactly maintained until the last two clusters even when only-half of the partitions are used. The previous subsection also used a subset of partitions when $y=0$ (all those with $n_1=0$) and the distribution is approximately a power law only for small-k values [see Fig. 3(b)].

For this model, the probability defined by Eq. (43) for even and odd permutations $Q_A^{\pm}(x=1)$ becomes $P_A^{\pm}(k,x=1)=1/A$ for $k=1$ to $A-2$. For $k=A-1$ and A, either $P_A^{\pm}(k=A-1,x=1)$ of $P_A^{\pm}(k=A,x=1)$ is zero and the other one is $2/A$. In other words,

$$P_A^{\pm}(k=A-1,x=1)+P_A^{\pm}(k=A,x=1)=2/A .$$

Here the probability for the size of $k=A-1$ or A, whichever is even (odd), is zero for even (odd) permutations and the other one is nonzero. This situation is the same as a die with $A-1$ faces. The number of dots on the $A-2$ faces are 1 to $A-2$, which are equally weighted with $1/A$. The last face has $A-1$ or A dots, whichever is odd (even) for even (odd) permutations. This face is weighted by $2/A$. We can also relate this to a die with A faces, with all faces equally weighted by $1/A$. In this case, the number of dots on the first $A-2$ faces are $k=1$ to $A-2$. The last two faces have the same number of dots either $k=A-1$ or A, which depends on whether A is even or odd and whether even or odd permutations are being considered. This is not a lopsided die, i.e., all the faces are weighted equally. But the numbers of dots on the faces are distributed differently from the usual die.

The cumulative mass [cf. Eq. (38)], defined by

$$M^{\pm}(s)=\sum_{j=1}^{[s]+1} j\langle n_j \rangle^{\pm} , \tag{72}$$

is shown for $A=10$ at $x=1$ in Fig. 3(c). We note that $M^{\pm}(s)$ is a uniform staircase function until the last two steps are reached. Then, for A even [Fig. 3(c)], an intermission appears as a double step at $s=A-2$ with a missing rise at $s=A-1$ (i.e., missing Ath step) in $M^{+}(s)$ and in $M^{-}(s)$ as a missing rise at $s=A-2$ with a double step at $s=A-1$. The same situation happens for the A odd case but with $M^{+}(s)$ and $M^{-}(s)$ interchanged.

F. Cayley's theorem and Gauss polynomials: The transformation to a state of dimers only

We next consider a very particular model in which all the x_k's are different, but the choice for each x_k is generated in a particular way. Namely, we take

$$x_k=\frac{1}{1-q^k} , \tag{73}$$

where q is a parameter whose range is $-1<q<1$ to keep x_k and n_k positive. For this particular choice, the partition function $Q_A(\mathbf{x})$ is again simple and is obtained by using a theorem due to Cayley [33]. Cayley's theorem for a decomposition is the following:

$$\frac{1}{(1-q)(1-q^2)\cdots(1-q^A)} = \sum_{\Pi_A} \frac{M_2(A,\mathbf{n})/A!}{(1-q)^{n_1}(1-q^2)^{n_2}\cdots(1-q^A)^{n_A}} , \tag{74}$$

with $M_2(A,\mathbf{n})$ the Cauchy's number of Eq. (7). The sum in Eq. (74) is over all partitions of A. Using this result, the partition function for the model is

$$Q_A(\mathbf{x})=A!\prod_{k=1}^{A} x_k=\frac{A!}{(1-q)(1-q^2)\cdots(1-q^A)} . \tag{75}$$

The ensemble-averaged n_k's can easily be obtained using the results of Sec. III and they are

$$\langle n_k \rangle = \left[\frac{x_k}{k}\right]\frac{x_1x_2\cdots x_{A-k}}{x_1x_2\cdots x_A}=\frac{x_k}{k\prod_{j=1}^{k}x_{A-j+1}} . \tag{76}$$

This result can be rewritten in terms of Gauss polynomials [33]. Defining

$$[q]_k=(1-q)(1-q^2)\cdots(1-q^k) , \tag{77}$$

then

$$\langle n_k \rangle = \frac{[q]_{k-1}}{k} \begin{bmatrix} A \\ k \end{bmatrix} , \tag{78}$$

where

$$\begin{bmatrix} A \\ k \end{bmatrix}$$

is a Gauss polynomial defined as $[q]_A/([q]_k[q]_{A-k})$.

Properties of the distribution of $\langle n_k \rangle$ are as follows. At $q=0$, which gives $x_k=1$ for all k as in Sec. IV A, $\langle n_k \rangle = 1/k$ and a scale invariant power law emerges. As $q \to 1$, $x_k = k^{-1} \lim_{q \to 1} (1-q)^{-1}$ by Eq. (73) and

$$\langle n_1 \rangle = A . \tag{79}$$

All other n_k's are zero, so that only monomers are present. The same results can be obtained at $x \to \infty$ from Sec. IV A also. The model has an interesting solution at $q \to -1$. Equation (73) gives $x_k = \frac{1}{2}$ for odd k and $x_k = k^{-1} \lim_{q \to -1} (1+q)^{-1}$ for even k. For A even,

$$\langle n_2 \rangle = \frac{A}{2} \tag{80}$$

and all other $\langle n_k \rangle$'s are zero. For A odd,

$$\begin{aligned} \langle n_1 \rangle &= 1 , \\ \langle n_2 \rangle &= \frac{A-1}{2} , \end{aligned} \tag{81}$$

and all other $\langle n_k \rangle$'s are zero. Thus, only clusters of size 2 (dimers) exist for even A. For odd A, only one monomer is present and all other clusters are dimers. The result of Eqs. (80) and (81) is an example of pairing phenomena and is an interesting solution for studying social behavior. A peak appears at the group size of two in a closed Vervet monkey troop and in the size of parties reserving at a restaurant [34]. The detailed comparison of the social behavior of monkeys and people with our various model predictions will be discussed in Sec. V. Pairing phenomena appear in various areas of physics.

G. Transitions to modes made of clusters with even number of elements only

In the last section, x_k was taken as $1/(1-q^k)$. Here we take $x_k = 1+q^k$ with $-1 \le q < \infty$ and generate another solution to illustrate the many possibilities which exist. For this choice of x_k, the generating function of Eq. (11) is

$$Q(u,\mathbf{x}) = [1/(1-u) - q/(1-qu)]/(1-q) .$$

The partition function $Q_A(\mathbf{x})$, with $\mathbf{x}=(1+q, 1+q^2, \cdots)$, can then be shown to be

$$Q_A(\mathbf{x}) = A! \frac{(1-q^{A+1})}{(1-q)} \tag{82}$$

from a result in Ref. [17]. This gives

$$\langle n_k \rangle = \left[\frac{1+q^k}{k} \right] \left[\frac{1-q^{A-k+1}}{1-q^{A+1}} \right] . \tag{83}$$

At $q=0$, $x_k=1$ for all k and $\langle n_k \rangle = 1/k$ as in Sec. IV A. As $q \to \infty$, $x_k = \lim_{q \to \infty} q^k$ and thus $\langle n_k \rangle = 1/k$. This large-$q$ limit corresponds to the case in which each constituent is weighted the same, independently of the cluster to which it belongs. Thus, the weight $x_k = q^k$ for the cluster of size k has no effect on the cluster distribution and becomes effectively the same as the $x=1$ case. This behavior has also been shown in Ref. [16].

At $q=-1$, $\mathbf{x}=(0,2,0,2,0, \ldots)$, so that the x_k for odd k's are zero and for even k's are 2. For even A

$$\langle n_k \rangle = \frac{2}{k} \tag{84}$$

for even k and $\langle n_k \rangle = 0$ for odd k. This case shows a scale invariance but with missing clusters of odd sizes. The cumulative mass $M(s)$ shows this situation well with missing rises at each position of even integer s, i.e., missing steps at each odd number of step position [see Fig. 3(d)]. In this case, the probability of Eq. (43) becomes $P_A(k, q=-1) = 2/A$ for even k and zero for odd k. Thus, this specific model can describe a die with $A/2$ faces with even number of dots on each faces of $k=2$ to A. All the $A/2$ faces are weighted equally by $2/A$.

For odd A, as $q \to -1$,

$$\langle n_k \rangle = \left[\frac{2}{k} \right] \left[\frac{A-k+1}{A+1} \right] \tag{85}$$

for even k, and

$$\langle n_k \rangle = \frac{2}{A+1} \tag{86}$$

for k odd. This case corresponds to a lopsided die and we lose the scale invariance. The cumulative mass $M(s)$ shows the position s dependences [see Fig. 3(d)].

V. APPLICATIONS TO VARIOUS SYSTEMS

In this section we will apply many of the results developed in the previous section to various phenomena. Applications cover such diverse areas as nuclear physics, astrophysics, population genetics and social behavior. Results will be compared to existing data.

A. The x model: Nuclear fragmentation, atomic ionization, and population genetics

In the x model of Sec. IV A, the quantity x contains the physical contents of the corresponding system. To illustrate this remark we consider an application of this model to the particular case of nuclear fragmentation produced by nuclear collisions. For example, a proton hitting a target nucleus will fragment the nuclear target. Similarly, a collision between two nuclei produce fragments of varying sizes. After the collision, the distribution of nuclear fragments or clusters is measured. In a statistical development of the fragmentation process, a weight is assigned to each possible partition of the fragmentation phenomena. The partitions are given by Eq. (2) subject to the constraint of Eq. (1) where the subscript j is the number of nucleons in the cluster of size j. A proton hitting a target made of 49 nucleons to make a combined system of 50 nucleons can produce a partition

$(1^4,4^2,6^1,7^2,9^2)$ which has four monomers or single nucleons, two mass 4 clusters, one mass 6 cluster, two mass 7 clusters, and two mass nine clusters (see Fig. 2). This partition is one of many possible fragmentations of the combined system with $A=50$ nucleons and the total number of possible fragmentations is given by $p(A)$ discussed in Sec. II, which becomes Eq. (4) for in a large-A limit. Each possible partition is then treated as a member of an ensemble of fragmentation schemes, and a resulting distribution of cluster sizes is obtained by ensemble averaging with a weight. The weight used in Ref. [14] is given by Eq. (10) with a single tuning parameter x; $x_j=x$ for all j.

Thermodynamic considerations developed in Refs. [14] and [16] give the following simple form for x involving the interplay of many different effects:

$$x=\frac{V}{v_0}e^{-a_v/k_BT}e^{-(k_BT/\varepsilon_0)T_0/(T+T_0)}. \tag{87}$$

The various quantities appearing in x are as follows. V is the freeze-out or equilibrium volume. This volume is the interaction volume of the collision in which the various processes take place that produce the various products of a nuclear collision. The quantity T is the freeze-out or equilibration temperature of the system. v_0 is the quantum volume given by $v_0=h^3(2\pi MK_BT)^{-3/2}$ and is a volume associated with a thermal de Broglie wavelength λ_T such that $v_0=\lambda_T^3$. In turn, $\lambda_T=h/P_T$, where $P_T=(2\pi MK_BT)^{1/2}$ is a characteristic momentum associated with particles with energies $E_T\sim k_BT\sim P_T^2/2M$. The quantity a_v is the binding-energy coefficient associated with a cluster. Specifically, the binding energy of a cluster made of k nucleons was taken to be of the simple form $E_B(k)=a_v(k-1)$. E_B is backshifted by 1 in k so that a single nucleon has no binding, i.e., $E_B(1)=0$. The binding energy per particle, $E_B(k)/k=a_v(1-k^{-1})$, saturates at a value a_v which can be taken as 8 MeV. $a_v=E_B(k)-E_B(k-1)$ is also the separation energy or work function which is the energy necessary to remove one nucleon from the cluster. ε_0 is the level spacing parameter with $\varepsilon_0=1/g_0$, where g_0 is the level density parameter discussed in Eq. (6). The quantity ε_0 relates to the spacing of excited levels in a cluster. $\varepsilon_0\sim 8$ MeV from experiment and this value is about $\frac{1}{2}$ the Fermi-gas value $\varepsilon_0=4E_F/\pi^2$, where E_F is the Fermi energy. T_0 is a cutoff temperature for internal excitations of a cluster.

From the above discussion, the single quantity x contains the interplay of many physical quantities which relate to the fragmentation process and which determine the final distribution of products resulting from a collision. x is treated as a parameter. Properties of the distribution of fragments produced in a collision are determined by the single parameter x. Specifically, Eq. (29) gives expressions for the distribution of fragment sizes in $\langle n_k\rangle$ and for the correlations of fragment sizes in $\langle n_k(n_k-1)\rangle$ and $\langle n_kn_j\rangle$.

Figure 4 illustrates a comparison of the x model versus experiment for the cluster size distribution function $\langle n_k\rangle$ for the case of Ne+Au$\rightarrow k+X$ at the beam energy of 2100 MeV per nucleon [35]. The solid line is the fit of the x model with $x=10$ for $A=200$. The prediction of our simple x model for $\langle n_k\rangle$ gives a good fit to the experimental data as can be seen from the figure (solid curve). This is comparable with the more complicated fit of Ref. [36] (dashed curve) having surface energy effects. Equation (87) shows that the temperature corresponding to $x=10$ is $T\approx 14$ MeV if we put $T_0=0$ and take the freeze-out volume V to be the same volume as a nucleus with $A=200$ nucleons with normal density. For a volume twice this size, the temperature would be 10 MeV. However, to extract a more accurate temperature for this reaction, a better treatment of the fragmentation volume and inclusion of degeneracy factors as discussed in Ref. [16] is required.

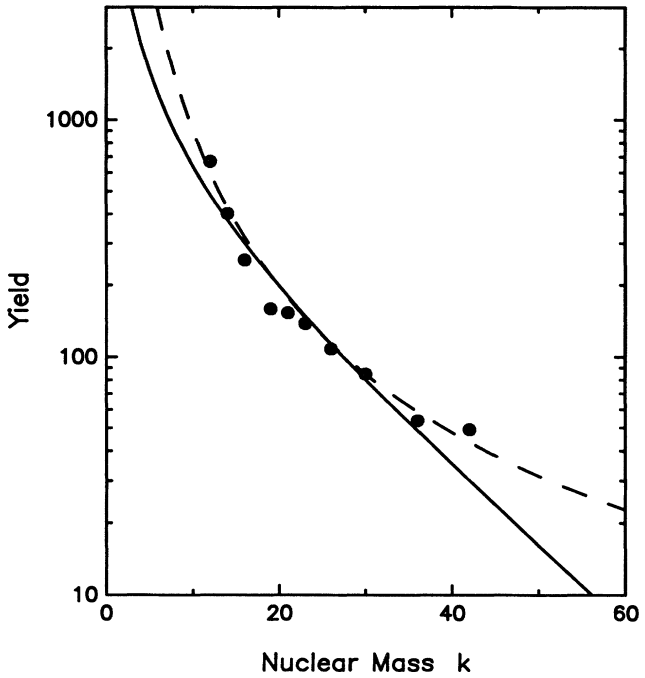

FIG. 4. Nuclear mass distribution in Ne+Au$\rightarrow k+X$ reactions at the beam energy of 2100 MeV per nucleon. The solid line is the fit of x model with $x=10$ for $A=200$. The solid circles are the data [35] and the dashed line is the fit of Ref. [36] having surface effects also.

As discussed in Ref. [14], the above choice of x when substituted into the Eq. (29) for $\langle n_k\rangle$ has the following interesting properties. For small x, the behavior of $\langle n_1\rangle$ is a result due to Fermi for the evaporation of a particle from a heated Fermi gas. Namely, $\langle n_1\rangle=(V/v_0)e^{-a_v/k_BT}$, where the exponential factor involving the work function or separation energy a_v acts as a barrier that inhibits evaporation. Replacing a_v by the ionization energy χ_r required to remove one electron from an r-times-ionized atom, the small-x behavior of $\langle n_1\rangle$ becomes the Saha equation [37,38] for ionization:

$$\langle n_1\rangle\sim\frac{n_{r+1}n_e}{n_r}=\frac{G_{r+1}g_e}{G_r}\frac{(2\pi m_ek_BT)^{3/2}}{h^3}e^{-\chi_r/k_BT},$$

where G_r and g_e are the so-called partition functions of the r-times-ionized atoms and the electron, respectively. n_r is the number density of r-times-ionized atoms and n_e is the number density of free electrons.

The large-x behavior of $\langle n_k \rangle$ is the Saha equation or law of mass action for abundances of species [14]. The large-x behavior of $\langle n_k \rangle$ can be written as

$$\frac{\langle n_k \rangle}{\langle n_1 \rangle} = \left[\frac{\langle n_1 \rangle v_0}{V} \right]^{k-1} e^{E_B(k)/k_B T} e^{b(k) k_B T T_0/(T+T_0)} , \tag{88}$$

where $E_B(k)=a_v(k-1)$ and $b(k)=(k-1)/\varepsilon_0$. The first exponential factor is the well-known Boltzmann binding-energy enhancement factor for cluster formation while the second exponential factor arises from internal excitations. Thus, evaporation of nucleons from a heated nuclear liquid, multifragmentation of a system into nucleons, and nucleons recombined into clusters can be described in terms of one underlying framework. This framework gives an expression for $\langle n_k \rangle$ whose limiting forms are the evaporation result and the cluster recombination result previously derived from independent thermodynamical considerations.

The x model also appears in population genetics. The population genetics model was developed by Ewens [24,25]. A comparison between the Ewens model and the fragmentation model is developed in detail in Ref. [26]. One aspect of population genetics is concerned with allelic partitions which measure genetic diversity. At the genetic level, different alleles or genes differ because of different DNA sequences. In a given sample of genetic material, many different alleles may exist and some alleles will have copies of themselves present in the sample. The genetic diversity distribution gives a relationship between the number of different types of alleles n_i, of which each type appears i times, versus the frequency of occurrences i. Thus, the partition $(1^4,4^2,6^1,7^2,9^2)$ of Fig. 2 in the genetic case represents four different alleles each appearing once, two different alleles each appearing four times, one type of allele appearing six times, two other types each appearing seven times, and finally two other types each appearing nine times. Here the total number of alleles in the sample is 50. The Ewens model assigns a weight to each possible genetic partition which is given by Eq. (10) with all the x_j's equal to a single parameter x. The correspondence between the nuclear cluster distribution produced in the fragmentation of a nucleus and the genetic diversity distribution of an allelic partition is as follows. The cluster size k becomes the number of copies of a given gene, while the number of clusters of size k, the n_k, becomes the number of different types of genes each having k copies as discussed in Ref. [25]. Thus, partitioning in this biological case is by different types of genes and by number of copies of these different types. By contrast, the fragmentation partitions are by size of the various clusters and by the number of clusters of a given size. The quantity $m=\sum n_j$, which is the multiplicity in the nuclear fragmentation case, becomes the total number of different types of genes present in the biological case. The quantity $A=\sum j n_j$ is the total number of genes present in the sample.

Just as the x in the nuclear case contains the physical quantities that determine the fragmentation behavior, the x in the genetic case contains the biological quantities that determine the genetic diversity. Namely, in population genetics, the x (called θ in Refs. [24] and [25]) is given by

$$\theta \equiv x = 4 N_e u \ . \tag{89}$$

N_e is the effective population size and the u is the mutation rate. N_e relates to the effects of genetic drift arising from the finite size of a population. Larger population size N_e has less genetic drift. Genetic drift tends to eliminate genetic diversity. By contrast, mutations enhance genetic diversity and the Ewens model assumes that every mutation produces a new allele not already present. An equilibrium, or more precisely, a steady state, is established between mutation and genetic drift. In the Ewens model the interplay between these two forces can be expressed in terms of a single parameter θ which plays a role similar to x in the fragmentation model. Small θ corresponds to very little genetic diversity with one type of gene having many copies of itself present in a sampling of a genetic material. Large θ corresponds to many different types of genes each appearing as singles or with few copies of themselves present. The genetic diversity distribution [24] are characterized by values of $\theta < 1$.

B. The x-y model: Solar element abundance

In the x-y model of Sec. IV D, the quantities x and y contain the physical contents of the corresponding system. Thermodynamic considerations developed in Ref. [16] give the following simple form for x and y involving the interplay of many different effects:

$$x = \frac{g}{h^3} (2\pi M)^{3/2} V (k_B T)^{3/2} , \tag{90}$$

$$y = \exp\left[-\frac{a_v}{k_B T} - \frac{k_B T}{\varepsilon_0} \left[\frac{T_0}{T+T_0} \right] \right] . \tag{91}$$

Here $g=4$ is the spin-isospin degeneracy and the binding energy for $k \neq 1$ is $E_B(k)=a_v k$ without backshifting in contrast to the x model case, Eq. (87), which uses a backshifted E_B. $E_B(1)$ is set equal to zero. Therefore, monomers are treated differently from other clusters by using $y \neq 1$. This model has been applied to a nuclear fragmentation process in Ref. [16].

A nuclear fragmentation is a breakup process of a large system. However, our model can also describe a clusterization process of A individuals such as a crystalization or condensation phenomena. As an example, we consider an application of the x-y model to a particular case in astrophysics, the solar element abundance [38]. Going from a finite nucleus to an astronomical system, the number of nucleons A and the volume of the system V become very large keeping the density $\rho = A/V$ finite; similar to taking a thermodynamic limit. As we will show

later in this section, in this limit, the relevant quantity which determines the distribution of cluster sizes is then the ratio

$$\frac{x}{A}=\frac{g}{\rho}\frac{(2\pi Mk_BT)^{3/2}}{h^3}\ , \tag{92}$$

where $\rho=A/V$ is the baryon density. Thus, x/A is an intensive quantity involving the density and temperature of a system. However, in the solar element abundance distribution, there is a cutoff for the cluster size since nuclei greater than $k\approx 250$ spontaneously fission. By restricting A to be $A=250$, we can account for this instability of very heavy nuclei. Correspondingly, the extensive quantities V and x will then reflect a system with this A. In using this procedure, we have divided a very large system where nucleosynthesis takes place in much smaller regions. Notice here that the range of nuclear force which is responsible for the nucleosynthesis is the order of fermi (10^{-13} cm) and the mean free path in a sun system is the order of angstrom (10^{-8} cm).

Figure 5 shows the fit of the x-y model with the maximum size of $A=250$ nucleons for the solar element abundance [38] formed through nucleosynthesis from free nucleons. This figure shows a good fit to the gross features of the data with $x\sim 40$ for masses up to the atomic mass of 120. The larger elements can be fitted with $x\sim 10$. The conditions of density and temperature or thermonuclear conditions that give this value of x are not well known. We therefore consider several cases. For the x value of ~ 40, Eq. (90) gives the temperature k_BT of 1 eV with the density ρ taken to be $3.3\times 10^{-11}\rho_0$, where ρ_0 is the nuclear matter saturation density. At

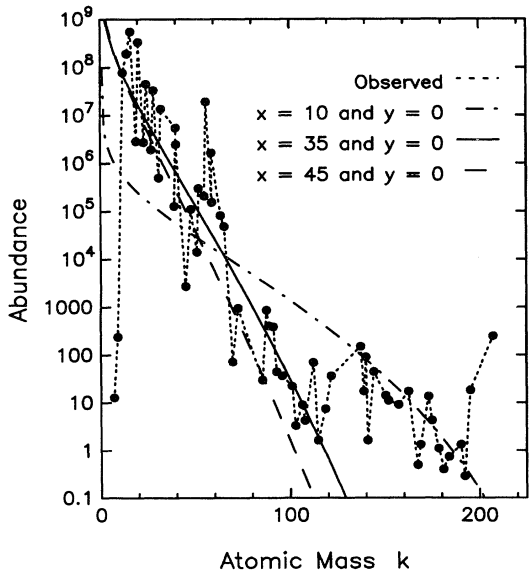

FIG. 5. The abundances of the elements in the solar system. The atomic mass distribution is converted from the atomic number distribution of Ref. [38]. The solid ($x=35$) and dashed ($x=45$) lines fit up to mass number of 120. The dash-dotted line ($x=10$) fit the larger mass region. In the fit, the maximum mass is set to $A=250$.

$k_BT\approx 1$ eV, the lower coexistence density for an infinite nuclear matter equation of state is the order of $10^{-11}\rho_0$. If we require the temperature to be $k_BT=1$ keV, then the density ρ is about $1.0\times 10^{-6}\rho_0$ for the x value of 40. The temperature $k_BT=1$ MeV requires the density to be $\rho=3.3\times 10^{-2}\rho_0$. For these temperature regions, Eq. (91) gives an almost zero value of y; even at $k_BT=1$ MeV, $y=1.3\times 10^{-7}$. It should be noted that our simple x-y model with Eqs. (90) and (91) is based on an equation of state having a zero-range nuclear interaction and does not have Coulomb or surface energy effects. Further refinement of this simple model is required to determine the actual condition, temperature and density, for element formation.

When x and A are large, i.e., in a thermodynamic limit with a large n_k, the cluster distribution function in the x model of Eq. (29) is simply [15]

$$\frac{\langle n_k\rangle}{A}\approx\frac{1}{k}\frac{x}{A}\left[1+\frac{x}{A}\right]^{-k}\ . \tag{93}$$

The relevant quantity which determines the distribution of cluster sizes is then the quantity $1/(1+x/A)$, where the ratio x/A is given by Eq. (92). The A in the previous paragraph was cutoff at $A=250$ to account for the fact that very heavy nuclei spontaneously fission and are thus not stable. The corresponding x which is determined with this A is then $x\approx 10$–45 (Fig. 5). However, the intensive quantity x/A is the relevant quantity in $\langle n_k\rangle$ for large A and this ratio is 0.1 for $x=25$ and $A=250$. This x/A can also reflect the x/A of the macroscopically much larger system where nucleosynthesis takes place. The quantity $1/(1+x/A)$ is 0.909 for $x/A=0.1$. It should be noted that the distribution $\langle n_k\rangle/A$ as given by Eq. (93) appears in Fisher's theory of species diversity [39]. Specifically, Fisher was able to fit the species diversity distribution of butterflies and moths using Eq. (93) where $\langle n_k\rangle$ is the number of types of butterflies with each type appearing k times in a sample. Again, as in the case of genetic diversity discussed in the previous subsection, the index k is changed from cluster size to frequency of occurrence for each type in going from the physical realm to the biological area [26]. Data on the butterfly distribution of Corbet and Williams [39] has $1/(1+x/A)=0.997\,4281$, i.e., $x/A=0.002\,5785$, which determines the distribution by Eq. (93).

C. Pairing phenomena and social behavior

Pairing phenomena appear not only in various areas of physics but are also quite common in social behavior. Social behavior can also be considered as a partitioning problem and can be studied using techniques developed in this paper. Then, instead of clusters made of nucleons, one investigates clusters or groups of individuals. However, the underlying forces responsible for the group structure in social behavior are less quantitatively understood than in nuclear fragmentation or in genetic diversity. In these later situations, the forces are associated with the thermodynamic variables, volume and temperature, and by binding energy and internal excitation effects

in the nuclear case, and by genetic drift and mutations in the biological case. Nevertheless, it is interesting to see if simple expressions can be found which fit data on social behavior based on the partitioning models developed in Sec. IV. For this purpose, we consider two pieces of data. One example is the social behavior of a troop of monkeys while the second example is the group structure of people reserving at a restaurant. For example, the partition $(1^4,4^2,6^1,7^2,9^2)$ of Fig. 2 considered in Sec. V A when discussing nuclear fragmentation and genetic diversity will now correspond to a group structure of four individuals, two groups of size four, one group of size six, two groups of size seven, and two groups of size nine. This partition is one of many possible arrangements of 50 individuals. A weight can next be given to each possible partition of the group, and the resulting distribution of group sizes can be obtained. These remarks will now be illustrated by comparing some of the results of Sec. IV with observed data on social behavior mentioned above.

Figure 6 illustrates the distribution of sleeping group sizes of a Vervet monkey troop [34] and some attempts to fit the distribution of group sizes. A truncated negative binomial [34], the x-y model of Sec. IV D, and the pairing model of Sec. IV F are compared with the data. The truncated negative binomial model of Cohen [34] gives the following ratio:

$$\frac{\langle n_{k+1}\rangle}{\langle n_k\rangle}=\left[\frac{k+r}{k+1}\right]q\ , \tag{94}$$

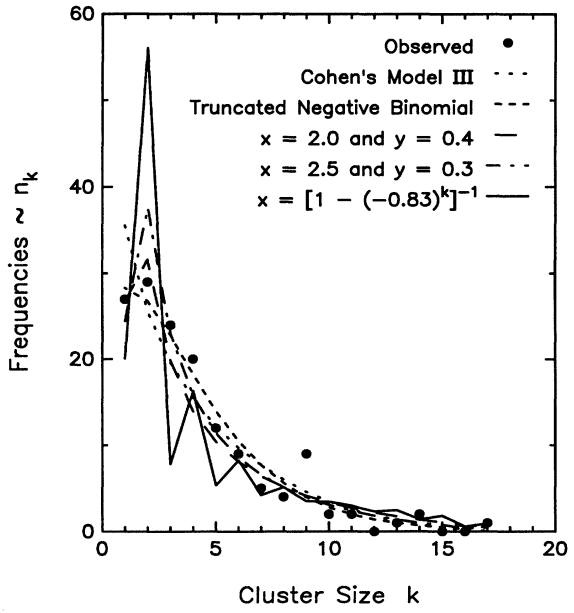

FIG. 6. Group size distribution of a closed Vervet monkey troop. Solid circles are for the observed values [34] and dotted and short-dashed curves are from Ref. [34] as discussed in the text. The solid line is the model of Sec. IV F with $q=-0.83$ and the long-dashed and dash-dotted lines are the x-y model of Sec. IV D with $x=2.0$ and $y=0.4$ or with $x=2.5$ and $y=0.3$, respectively. Here $A=17$ and the frequencies $\mathcal{N}n_k$ are normalized to $\mathcal{N}\sum_k kn_k=599$ which is the same as the data.

where r and $q=1-p$ are the parameters of the negative binomial distribution, r represents the growing rate of a group size, and q represents the decreasing rate of a group size. Cohen also considers a model (model III in Ref. [34]) where this ratio is given by

$$\frac{\langle n_{k+1}\rangle}{\langle n_k\rangle}=\left[\frac{k+r}{k+1}\right]\left[\frac{A-k}{(M-1)r+A-k-1}\right]\ . \tag{95}$$

The parameter r is the same as in Eq. (94) and the parameter M is the maximum number of groups allowed independent of the size A. While, no simple relationship exists for $\langle n_{k+1}\rangle/\langle n_k\rangle$ in our x-y model, the x model of Sec. IV A has

$$\frac{\langle n_{k+1}\rangle}{\langle n_k\rangle}=\left[\frac{k}{k+1}\right]\left[\frac{A-k}{x+A-k-1}\right]\ . \tag{96}$$

Comparing Eq. (95) with Eq. (96), we see that model III of Cohen would reduce to the x model result when $(M-1)r\to x$ and $r\to 0$, which implies that $M\to\infty$. On the other hand, Eq. (95) reduces to Eq. (94) for a finite k when $A\to\infty$ and $M\to\infty$ with finite value of $Mr/A=(1-q)/q$. We will come back to these comparisons later in this section. However, we note here that the truncated negative binomial model Eq. (94) is for an open system with $A\to\infty$, and model III and the x model are for a closed system with a fixed finite A. The x model does not fit the data very well because it does not suppress the individuals $(k=1)$ compared to the pair $(k=2)$. Otherwise (for $k>2$), the x model fit is quite similar to the x-y model fit with the same x value. The truncated negative binomial fit of Cohen shown in Fig. 6 (short-dashed curve) has $r=1.92$ and $p=1-q=0.35$ while model III (dotted curve) has $r=0.64$ and $M=6$. These values of r and M give $(M-1)r=3.2$, which is comparable to the x values of x-y model fits. All models give essentially the same behavior for large group sizes, i.e., with $k>8$.

The peak at group size $k=2$ appearing in the monkey data of Fig. 6 reflects a common characteristic of social behavior. The x-y model of Sec. IV D fits the qualitative features of the data and can even account for the peak when y is taken less than 1 [15]. The negative binomial fit of Ref. [34] does not peak at $k=2$ while it is better than model III for small $k<5$. We feel that the peak at the $k=2$ pair is a very important aspect of social behavior and obtaining it is a very important feature of any model. The pairing model of Sec. IV F oscillates with peaks at even integers and valleys at the odd integers. The troop data of Fig. 6 does not have these oscillations. However, the behavior of people reserving at a restaurant [34] as shown in Fig. 7 shows such oscillations between even and odd group sizes and has a strong suppression of singles. The model of Sec. IV G, which considers the clusters with even number of elements, can also account for this oscillating behavior and the suppression of singles. Also shown is the x-y model fit to the data. While all three models fit the overall behavior of the size distribution of parties, the pairing model of Sec. IV F best fit the oscillating behavior. The variable q in $x_k=(1-q^k)^{-1}$, Eq. (73), accounts for the strength of pairing. Further study of q

may reveal the underlying forces responsible for the pairing in social behavior.

As we have seen previously in comparing Eqs. (94)–(96) to each other, our model and Cohen's model are closely related. Cohen's model III, which is based on Kingman's Markov chain model [40], is compared with our x model. Cohen's model III (Eq. (11a) of Ref. [34]) gives

$$G(k)=MP(k) =M\begin{bmatrix}-r\\k\end{bmatrix}\begin{bmatrix}-(M-1)r\\A-k\end{bmatrix}\Big/\begin{bmatrix}-Mr\\A\end{bmatrix}, \quad (97)$$

where we have changed the notation used by Cohen to our notation; $s\to k$, $k\to M$, and $n\to A$. Here we first note that $G(k)/M$ is a Polya-Eggenberger distribution [30]. The Polya-Eggenberger distribution can be obtained from an urn model with two colored balls. Initially the urn contains R red balls and G green balls. Each time a ball is drawn, the drawn ball and S additional balls of the same color are replaced. The probability in n trials of obtaining m red balls is then [30]

$$P_n(m,\alpha,\beta)=\begin{bmatrix}-\alpha\\m\end{bmatrix}\begin{bmatrix}-\beta\\n-m\end{bmatrix}\Big/\begin{bmatrix}-(\alpha+\beta)\\n\end{bmatrix}, \quad (98)$$

where $\alpha=R/S$ and $\beta=G/S$. These α and β are the initial number of red and green balls in the unit of S. $P_n(m,\alpha,\beta)$ can also be written as

$$P_n(m,\alpha,\beta)=\begin{bmatrix}n\\m\end{bmatrix}\frac{B(\alpha+m,\beta+n-m)}{B(\alpha,\beta)}. \quad (99)$$

$B(a,b)$ is a β function given by Eq. (46). Here $(\alpha+m)S=R+mS$ is the total number of red balls in the urn after n trials and $(\beta+n-m)S=G+(n-m)S$ is the total number of green balls after n trials. Comparing the Polya-Eggenberger distribution with Cohen's model III, we obtain $\alpha=R/S=r$, $\beta=G/S=(M-1)r$, $n=A$, and $m=k$. Thus, the parameter $r=\alpha$ in Cohen's model III corresponds to the initial number of red balls divided by the number of additional balls added each time (S). M is the ratio of the initial number of total balls ($R+G$) to the number of red balls (R).

The distribution $P_A(k,x)=k\langle n_k\rangle/A$ of Eq. (45) in the x model is also a Polya-Eggenberger distribution [29] with $\alpha=R/S=1$, $\beta=G/S=x$, $n=A-1$, and $m=k-1$. Condition $\alpha=1$ gives $R=S$ and $x=\beta=G/R$. In Cohen's model III, $r=\alpha=0.64$ and $M=6$ which give $x=\beta=(M-1)r=3.2$.

The Cohen result Eq. (97) for $G(k)$ in the limit $M\to\infty$ and $r\to 0$ with finite $Mr\to x$ gives

$$G(k)=\begin{bmatrix}A\\k\end{bmatrix}\frac{x\Gamma(x+A-k)\Gamma(k)}{\Gamma(x+A)}, \quad (100)$$

which is the $\langle n_k\rangle$ in the x model. Thus, a strong similarity exists between model III and our x model. As can be seen in the generating function $Q(u,x)$ of Eq. (11) for the partition function $Q_A(x)$, $M=\infty$ in our x model. The multiplicity M is the power of the Mth order expansion term of the exponential generating function $Q(u,x)$ of Eq. (11). The limit $M\le A$ only exists when we consider A fixed. Both model III and the x model can be viewed as a distribution of A objects among M indistinguishable boxes allowing for empty boxes. Here a weight to each specific distribution is assigned by the parameter r or x. Cohen's model III has a finite number of boxes M which is less than the number of objects A in contrast to the x model in which there is no limit on the number of boxes M. Also the number of parameters in the Cohen's model III is reduced from two (r and M) to one (x) in taking the above limit $M\to\infty$ and $r\to 0$ with $Mr\to x$.

The x and y quantities relate the underlying behavior of the fragmentation process to volume, temperature, binding energy, and level density effects. In population genetics, the corresponding quantity involves the balance between genetic drift and mutations. Cohen's model III is a stationary distribution in which a balance exists for the arrivals and departures of monkeys from one group to another without a change in the total number of monkeys (closed system). The truncated negative binomial model considers such a balance and also allows for the birth and death of monkeys in the troop (open system).

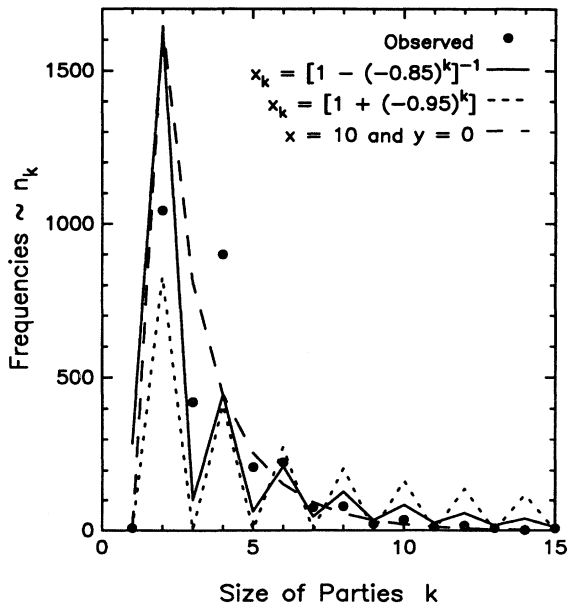

FIG. 7. Size distribution of parties of people reserving at a restaurant [34]. The solid line is the pairing model of Sec. IV F, the dotted line is the even cluster model of Sec. IV G, and the dashed line is the x-y model of Sec. IV D. These fits are with $A=20$ and the normalization condition of $\mathcal{N}\sum_{k=1}^{15}k\langle n_k\rangle=11\,614$, which is the same as the data.

VI. CONCLUSION

We have shown that simple models of fragmentation and partitioning phenomena can be developed which show a rich spectrum of different types of behavior. The models considered here are based on a correspondence between clusters and partitions with cycles of the permutation group. Methods from combinational analysis are used to obtain analytic expressions for canonical ensembles. These canonical ensembles are then used to obtain

exactly soluble models of fragmentation and clusterization phenomena and other types of partitioning problems. Properties of the distribution of cluster and group sizes are studied.

A wide range of fragmentation behavior can be obtained from these models depending on the choice of tuning parameters. In some cases, exact scale invariant hyperbolic power laws emerge in the distribution of cluster or group sizes. Situations in which no monomers exist and in which only pairs exist are also studied. One model developed, which is based on a theorem due to Cayley, has the interesting property of having only dimers or pairs present at a particular point. Other situations are discussed. Various properties of the distribution of cluster and group sizes are given. Simple expressions are found for moments, correlations, and fluctuations of the distribution of cluster sizes. Fragmentation and clusterization phenomena are also related to simple probability pictures based on coin and dice models developed in information theory.

Section V gives some applications of the results developed in Sec. IV to some specific problems in the physical, biological, and social sciences. The distribution of cluster sizes resulting from a nuclear collision is accounted for in terms of a simple soluble model. Another application of our approach is to the solar abundance of the elements. An interrelationship between nuclear fragmentation and Ewens theory of genetic diversity in biology was noted. An application of the approach to the social behavior of monkeys and of people was also given.

ACKNOWLEDGMENTS

This work was supported in part by National Science Foundation Grant No. 89-03457 and by Rutgers University and by the U.S. Department of Energy.

APPENDIX: GENERATING FUNCTIONS FOR PARTITIONS

The generating function for $p(A)$ [18] is

$$P(u)=\frac{1}{(1-u)(1-u^2)(1-u^3)\cdots}=\prod_{i=1}^{\infty}\left[\frac{1}{1-u^i}\right]=\sum_{A=0}^{\infty}p(A)u^A . \tag{A1}$$

Since $-\ln(1-x)=\sum_{n=1}^{\infty}x^n/n$ and $\sum_{n=1}^{\infty}x^n=x/(1-x)$, $P(u)$ can be written as $e^{f(u)}$ where

$$f(u)=\sum_{n=1}^{\infty}\frac{u^n}{n(1-u^n)} \tag{A2}$$

for $u^2<1$. Using $\sum_{n=1}^{\infty}1/n=0.577\,21+\lim_{n\to\infty}\ln n$ and $\sum_{n=1}^{\infty}1/n^2=\pi^2/6$, it is easy to show that, near $u=1$,

$$f(u\approx 1)\approx(\pi^2/6)(1-u)^{-1}-\tfrac{1}{2}\lim_{n\to\infty}\ln n+\beta ,$$

with β a constant of the order of unity. The steepest-descent contour integration, i.e., $P(u_0)=e^{f(u_0)}\approx p(A)u_0^A$, where u_0 is such that $d[f(u)-A\ln u]/du=0$ at $u=u_0$, leads to Eq. (4) up to an unimportant numerical factor.

The enumerating function for $p(A,m)$ is a two-variable function [41]

$$P(u,t)=\frac{1}{(1-tu)(1-tu^2)(1-tu^3)\cdots}=\prod_{i=1}^{\infty}\left[\frac{1}{1-tu^i}\right]=\sum_{m=0}^{\infty}P(u,m)t^m , \tag{A3}$$

with $P(u,m)$ a generating function for partitions with m parts which is

$$P(u,m)=\sum_{A=0}^{\infty}p(A,m)u^A=\frac{u^m}{(1-u)(1-u^2)\cdots(1-u^m)} . \tag{A4}$$

Again the steepest-descent method leads to Eq. (5).

Other quantities of interest in partition enumeration are the following. The division of A into factors such that no n_i is greater than 1 is defined by a symbol $q(A)$. $q(A)$ is generated by [18]

$$Q(u)=(1+u)(1+u^2)(1+u^3)\cdots=\prod_{i=1}^{\infty}(1+u^i)=\sum_{A=0}^{\infty}q(A)u^A . \tag{A5}$$

If different orderings are allowed, as in $5=4+1=1+4=\cdots$, the number of partitions $r(A)$ is obtained from a generating function $R(u)$ given by [16]

$$R(u)=\frac{1-u}{1-2u}=\sum_{A=0}^{\infty}r(A)u^A . \tag{A6}$$

$p(A)$, $q(A)$, and $r(A)$ all have polynomial generating functions. In contrast, the cycle indicators have an exponential generating function as shown by Eq. (11) in Sec. III. A more general generating function than the one considered in Sec. III is given in Ref. [16].

*Permanent address: Department of Physics and Astronomy, Rutgers University, Piscataway, NJ 08855.
†Electronic address: sjlee@ruthep.rutgers.edu.

[1] J. E. Finn *et al.*, Phys. Rev. Lett. **49**, 1321 (1982).
[2] G. S. Hawkins, Annu. Rev. Astron. Astrophys. **2**, 149 (1964).
[3] B. Gutenberg and C. F. Richter, Ann. Geophys. **9**, 1 (1956).
[4] L. Kadanoff, S. Nagel, L. Wu, and S. Zhou, Phys. Rev. A **39**, 6524 (1989).
[5] P. Bak, C. Tang, and K. Wiesenfeld, Phys. Rev. Lett. **59**, 381 (1987); Phys. Rev. A **38**, 364 (1988).
[6] W. K. Hartmann, Sci. Am. (January), 84 (1977).
[7] D. Stauffer, *Introduction to Percolation Theory* (Taylor & Francis, Philadelphia, 1985).
[8] M. E. Fisher, Physics (N.Y.) **3**, 255 (1967).

[9] G. Zipf, *Human Behavior and the Principle of Least Effort* (Hafner, New York, 1972).
[10] V. Pareto, *Cours d'Economie Politique,* Lausanne, 1897.
[11] W. H. Press, Commun. Mod. Phys. C 7, 103 (1978); P. Dutta and P. M. Horn, Rev. Mod. Phys. **53**, 497 (1981).
[12] B. B. Mandelbrot, *The Fractal Geometry of Nature* (Freeman, San Francisco, 1982).
[13] E. W. Montroll and B. J. West, in *Fluctuation Phenomena,* edited by E. W. Montroll and J. L. Lebowitz (North-Holland, Amsterdam, 1976), p. 61.
[14] A. Z. Mekjian, Phys. Rev. C **41**, 2103 (1990); Phys. Rev. Lett. **64**, 2125 (1990).
[15] S. J. Lee and A. Z. Mekjian, Phys. Lett. A **149**, 7 (1990).
[16] S. J. Lee and A. Z. Mekjian (unpublished).
[17] J. Riordan, *An Introduction to Combinational Analysis* (Wiley, New York, 1958).
[18] M. Abramowitz and I. Stegun, in *Handbook of Mathematical Functions,* Natl. Bur. Stand. Appl. Math. Ser. No. 55, edited by M. Abramowitz and I. Stegun (U.S. GPO, Washington, D.C., 1965).
[19] A. Bohr and B. R. Mottelson, *Nuclear Structure* (Benjamin, New York, 1969), Vol. I.
[20] J. J. Griffin, Phys. Rev. Lett. **17**, 478 (1966).
[21] D. Mitchell and N. Turok, Phys. Rev. Lett. **58**, 1577 (1987).
[22] R. Hagedorn, in *Cargese Lectures in Physics,* edited by E. Schatzman (Gordon and Breach, New York, 1973), Vol. 6, p. 643.
[23] M. Hamermesh, *Group Theory and its Application to Physical Problems* (Addison-Wesley, Reading, MA, 1962).
[24] W. J. Ewens, Theor. Popul. Biol. **3**, 87 (1972).
[25] W. J. Ewens, *Mathematical Population Genetics* (Springer-Verlag, Berlin, 1979).
[26] A. Z. Mekjian, Phys. Rev. A (to be published).
[27] K. K. Gudima and Y. A. Murin, Phys. Lett. B **234**, 1 (1990).
[28] H. R. Jaqaman, G. Papp, and D. H. E. Gross, Nucl. Phys. A **514**, 327 (1990).
[29] A. Z. Mekjian (unpublished).
[30] W. Feller, *An Introduction to Probability Theory and Its Applications* (Wiley, New York, 1957), Vols. 1 and 2.
[31] J. S. Rowlinson, Nature **225**, 1196 (1970).
[32] E. T. Jaynes, in *The Maximum Entropy Formalism,* edited by D. Levine and M. Tribus (MIT, Cambridge, MA, 1979), p. 15.
[33] G. E. Andrews, *Theory of Partitions* (Addison-Wesley, Reading, MA, 1976).
[34] J. E. Cohen, *Casual Groups of Monkeys and Man* (Harvard University, Cambridge, MA, 1971); Theor. Popul. Biol. **3**, 119 (1972).
[35] A. I. Warwick *et al.*, Phys. Rev. C **27**, 1083 (1983).
[36] A. L. Goodman, J. I. Kapusta, and A. Z. Mekjian, Phys. Rev. C **30**, 851 (1984).
[37] M. N. Saha, Philos. Mag. **40**, 472 (1920).
[38] D. D. Clayton, *Principles of Stellar Evolution and Nucleosynthesis* (McGraw-Hill, New York, 1968).
[39] R. A. Fisher, A. S. Corbet, and C. B. Williams, J. Anim. Ecol. **12**, 42 (1943).
[40] J. F. C. Kingman, J. Appl. Probability **6**, 1 (1969).
[41] H. Gupta, *Royal Society Mathematical Tables* (Cambridge University, Cambridge, 1958), Vol. 4.